

Ingrid Espmark Wibe

Power Flow Tracing for Norwegian Offshore Electrification

Master's thesis in Energy and Environmental Engineering

Supervisor: Steve Völler

Co-supervisor: Vijay Venu Vadlamudi

June 2021

NTNU
Norwegian University of Science and Technology
Faculty of Information Technology and Electrical Engineering
Department of Electric Power Engineering

Ingrid Espmark Wibe

Power Flow Tracing for Norwegian Offshore Electrification

Master's thesis in Energy and Environmental Engineering
Supervisor: Steve Völler
Co-supervisor: Vijay Venu Vadlamudi
June 2021

Norwegian University of Science and Technology
Faculty of Information Technology and Electrical Engineering
Department of Electric Power Engineering



Norwegian University of
Science and Technology

Abstract

It is generally known that in power systems with more than one supplier and one consumer, electric power cannot be physically traced. Janusz Bialek explained this by saying that it is "impossible to 'dye' the incoming flows (to a node) and check the colour of the outflows". With Power Flow Tracing (PFT) it is possible to theoretically trace the electric power, and by that give estimations of how energy flows from specific generators to specific loads. Before performing PFT on a power system there is need for a power flow analysis or historical measured values. PFT can be used for e.g. transmission service pricing, efficient use of load shedding and CO₂-emission apportioning. The latter is becoming very relevant due to the climate changes and global warming, it could improve knowledge about how power consumption affect the emission of greenhouse gases.

In this Master's thesis a model based on PFT has been developed in the programming language Python. The model, which is confidential and meant for in-house use at NTNU, is called the PFT Model. It both calculates generators and loads contribution to the power system, and visualises the results in a map of Europe. It was demonstrated on scenarios with offshore electrification in Norway. The power flow analysis of these scenarios, which provided the input data to the PFT Model, was done in EMPS in the specialisation project. The scenarios included two degrees of electrification of offshore platforms: full and partial, and they were set to year 2025.

The results from simulations with the PFT Model revealed how energy would flow to and from installations on the Norwegian continental shelf, if they were to be electrified. Even though some of the imported power was found to be produced with CO₂-dense coal, the total emission associated with the platforms would be reduced with electrification. Seasonal and daily variations that impact the power system, e.g. most wind in the winter and most power demand during the day, were discovered and explained as well. With these sensible results, and an assessment of limitations, it was concluded that the PFT Model was successful.

Sammen drag

Det er generelt kjent at elektrisk kraft ikke kan spores fysisk i kraftsystemer med mer enn én leverandør og én forbruker. Janusz Bialek forklarte dette med å si at det er "umulig å 'fargelegge' innkommende strømmer (til en node) og sjekke fargen på utstrømmingene". Med Power Flow Tracing (PFT, kraftflyt-sporing på norsk) er det mulig å teoretisk spore den elektriske kraften, og med det gi estimater av hvordan energi strømmer fra spesifikke generatorer til spesifikke laster. Før gjennomføring av PFT på et kraftsystem er det behov for en kraftflytanalyse eller historiske måleverdier. PFT kan brukes til f.eks. prissetting av overføringstjenester, effektiv bruk av lastreduksjon og fordeling av CO₂-utslipp. Sistnevnte blir veldig relevant på grunn av klimaendringene og global oppvarming, det kan forbedre kunnskapen om hvordan strømforbruk påvirker utslipp av klimagasser.

I denne masteroppgaven har det blitt utviklet en modell basert på PFT i programmeringsspråket Python. Modellen, som er konfidensiell og ment for intern bruk på NTNU, ble kalt PFT-modellen. Den beregner både generatorer og laster sine bidrag til kraftsystemet, og visualiserer resultatene på et kart av Europa. Den ble demonstrert på scenarier med offshore elektrifisering i Norge. Kraftflytanalysen av disse scenariene, som ga inngangsdata til PFT-modellen, ble gjort i EMPS i spesialiseringsprosjektet. Scenariene inkluderte to grader av elektrifisering av offshoreplattformer: hel og delvis, og de ble satt til år 2025.


Resultatene fra simuleringer med PFT-modellen avslørte hvordan energi ville strømme til og fra installasjoner på den norske kontinentalsokkelen, hvis de skulle blitt elektrifisert. Selv om det ble funnet at noe av den importerte kraften ble produsert med CO₂-intens kull, ville det totale utslippet knyttet til plattformene blitt redusert med elektrifisering. Sesongbaserte og daglige variasjoner som påvirker kraftsystemet, f.eks. mest vind om vinteren og mest kraftbehov om dagen, ble også oppdaget og forklart. Med disse fornuftige resultatene, og en vurdering av begrensninger, ble det konkludert med at PFT-modellen var vellykket.

Preface

With this Master's thesis I conclude my degree within Energy and Environmental Engineering at NTNU. I am grateful for the time I have had at NTNU and in Trondheim, for all that I have learned and everyone I have had the pleasure to get to know.

I would like to give a special thanks to my supervisor Associate Professor Steve Völler for impeccable guidance throughout my final year. His calm and structural way of following up his students has been appreciated, and this thesis would not have been the same without him. I would also like to thank my co-supervisor Associate Professor Vijay Venu Vadlamudi for helpful insights in the theme of Power Flow Tracing. Throughout the process of this thesis the Master's thesis of Kjersti Berg has been a useful source of inspiration, which I want to acknowledged as well.

This degree would have been much harder without the continued support from my family and friends, so finally I want to thank all of them for always keeping my spirits up.



Ingrid Espmark Wibe

Trondheim, June 2021

Contents

Abstract	i
Sammendrag	ii
Preface	iii
List of Abbreviations	vi
List of Figures	viii
List of Tables	ix
1 Introduction	1
1.1 Motivation	1
1.2 Contributions	2
1.3 Organisation of thesis	3
2 Background	4
2.1 Impact of offshore electrification in Norway	4
2.1.1 Electrification of offshore oil and gas operations	4
2.1.2 The EMPS model	5
2.1.3 Scenarios	8
2.1.4 Main results from simulations	9
2.2 Power Flow Tracing (PFT)	12
2.2.1 Proportional Sharing Principle (PSP)	14
2.2.2 PFT algorithms using PSP	15
2.2.3 Bialek's algorithm	15
3 Applied Methodological Approach	22
3.1 Development of the Power Flow Tracing (PFT) Model	22
3.1.1 Input to the model	22
3.1.2 Choosing algorithm	23
3.1.3 Implementation of algorithm in Python	23
3.1.4 Verification and validation	28
3.2 Limitations in the method	33

3.2.1	Proportional Sharing Principle	33
3.2.2	Equivalent power systems	33
3.2.3	Local handling of loads	34
3.3	Simulations with the PFT Model	34
3.3.1	Yearly and hourly flow to offshore installations in Norway	35
3.3.2	Yearly and hourly flow from offshore installations in Norway	37
4	Results and Discussion	40
4.1	Yearly average	40
4.1.1	Full electrification versus partial electrification	43
4.2	Seasonal and daily variation	46
4.2.1	CO ₂ -coefficient in exporting areas	50
4.3	Discussion	51
4.4	Impact of results	52
4.4.1	Building of scenarios	52
4.4.2	Alternative usage of offshore wind power	52
4.4.3	Disadvantages for geographical positions	54
5	Concluding Remarks	56
5.1	Summary of results	56
5.2	Future work	57
5.2.1	Reactive Power Flow Tracing	57
5.2.2	Different scenarios	58
5.2.3	Parallel lines	58
5.2.4	Universal code	59
	References	60
	Appendices	63
	A Background data	64
	B Six Bus Test System	71
	C Power flow to/from offshore installations in Norway	73
	D Imported power to NCS4-A and CO₂-coefficients	78
	E The PFT Model	80

List of Abbreviations

- 450** WEO “450 ppm” scenario
- CHP** Combined Heat and Power
- CO₂** Carbon dioxide
- CP** WEO “Current Policy” scenario
- EMPS** EFT’s Multi-area Power-market Simulator
- GHG** Greenhouse Gases
- GOs** Guarantees of Origin
- KCL** Kirchhoff’s Current Law
- NCS** Norwegian Continental Shelf
- NP** WEO “New Policy” scenario
- PFT** Power Flow Tracing
- PSP** Proportional Sharing Principle
- TSO** Transmission System Operator
- WEO** World Energy Outlook

List of Figures

2.1	The EMPS 3 Model - Model of the European energy system with offshore areas.	6
2.2	Comparison of total emission of CO ₂ -equivalents in different scenarios. . .	10
2.3	Area prices in NO ₁ , NO ₃ and NO ₄ for scenarios with partial- and full electrification in 2025.	11
2.4	Guarantees of Origin[20].	13
2.5	Conceptual diagram for usage of the PFT method[22].	13
2.6	Proportional sharing principle[4].	14
3.1	Conceptual diagram for usage of the PFT method, starting with EMPS and assuming local handling of loads.	23
3.2	Illustration of power flow from France in full electrification scenario, using upstream-looking algorithm.	26
3.3	Illustration of power flow to Italy in full electrification scenario, using downstream-looking algorithm.	27
3.4	Illustration of power flow from Finland in base case, using upstream-looking algorithm.	28
3.5	Six bus test system[22].	29
3.6	Yearly average flow towards NCS4-A.	35
3.7	Flow towards NCS4-A in the winter.	36
3.8	Flow towards NCS4-A in the summer.	36
3.9	Yearly average flow from NCS4-B.	37
3.10	Flow from NCS4-B in the winter.	38
3.11	Flow from NCS4-B in the summer.	38
4.1	Total imported power to platforms on the NCS in the full electrification scenario, obtained by using net flow.	41
4.2	Total imported power to platforms on the NCS in the full electrification scenario, obtained by using gross flow.	42

4.3	Yearly average imported energy to NCS4-A, separated into contributing areas, in the full electrification scenario.	43
4.4	Overview of energy consumed, and its associated emission, in NCS4-A for full- and partial electrification.	44
4.5	Difference between the full- and partial electrification scenarios, in yearly average imported power to NCS4-A, separated into contributing areas. . .	45
4.6	Difference in export from areas contributing to NCS4-A, full- vs partial electrification.	46
4.7	Imported energy to NCS4-A on January 1 st , separated into contributing areas.	47
4.8	Imported energy to NCS4-A on July 1 st , separated into contributing areas.	48
4.9	Export from NO1 in the day (left) and night (right) on July 1 st	49
A.1	Production mix: Base case in 2025 (left) and full electrification in 2025 (right).	66
A.2	Production mix: Partial electrification in 2025.	67
A.3	Difference in production mix: Base case vs full electrification in 2025 (left) and Partly vs full electrification in 2025 (right).	68
A.4	Power exchange with neighbour areas in base case scenario in 2025.	69
A.5	Power exchange with neighbour areas in partial electrification scenario in 2025.	69
A.6	Power exchange with neighbour areas in full electrification in 2025.	70
C.1	Yearly average flow towards NCS1-A.	73
C.2	Yearly average flow towards NCS2-A.	74
C.3	Yearly average flow towards NCS3-A.	74
C.4	Yearly average flow towards NCS5-A.	75
C.5	Yearly average flow from NCS1-B.	76
C.6	Yearly average flow from NCS2-B.	76
C.7	Yearly average flow from NCS3-B.	77
C.8	Yearly average flow from NCS5-B.	77

List of Tables

2.1	Transmission capacity from shore in 2022[12].	5
2.2	Areas in the EMPS 3 Model.	7
2.3	Overview of scenarios.	9
2.4	Average area prices in Norwegian areas in base case and full electrification in 2025.	12
3.1	Results from applying the upstream-looking algorithm with gross flow on the Six bus test system.	31
3.2	Validation of the PFT code using base case.	32
4.1	CO ₂ -coefficients [ton/GWh].	50
4.2	Difference in production, consumption, import and export [GWh] between SINTEFs wind scenario and base scenario[33].	53
A.1	Energy consumption in areas with oil fields.	64
A.2	Installed power capacity in areas with gas turbines.	64
A.3	Installed power capacity in areas with offshore wind turbines.	65
B.1	Contribution of generators to loads.	71
B.2	Contribution of generators to lines.	72
B.3	Allocation of loss to loads.	72
D.1	Contributing areas to yearly average energy imported, and its associated emission, to NCS4-A in full- and partial electrification.	78
D.2	Yearly average CO ₂ -coefficients [ton CO ₂ /GWh] in partial- and full electrification.	79

Chapter 1

Introduction

1.1 Motivation

In a complex power transmission network, such as the European power system, it exists several possible routes where the electric power can flow from source to sink. The sources are generators, producing power from e.g. hydro, coal and wind. The sinks, also referred to as loads, are consuming units such as industries and private homes. There must be an instant balance between sources and loads, since electricity cannot itself be stored. Any action in one part of the power system, such as changing transfer capacity or altering the magnitude of a source or a load, can potentially alter the whole system.

Before the 1990, which was when the deregulation trend started, the European energy system consisted typically of public owned utilities. The utilities had a monopolistic position in their respective areas. After 1990, however, the electricity market became more competitive because of privatisation and deregulation. Deregulation of an energy system is to restructure it such that generation and sales are subject to competition[1]. In Norway, and later the other Nordic countries, the Energy Act of 1990 made sure that the power systems were "conducted in a way that efficiently promotes the interests of society."[2]. Market efficiency is dependent on transparency from both producers and consumers[3].

It is generally known that it is not possible to physically trace electricity back to its source in power systems with more than one generator and one load. With a monopolistic market the measures for theoretically tracing the power from source to load was of little interest. With the deregulation of the power systems, aspects such as transmission service pricing and loss allocation became interesting in order to improve transparency and by that system efficiency[4]. Also, with the climate changes and global warming, in-

formation about how electricity usage affects emission of greenhouse gases (GHG), have become more requested.

Statistics Norway (SSB) publishes yearly statistics about emissions connected to energy production in Norway, and does not take into account potential import and export of power[5]. The Norwegian Water Resources and Energy Directorate (NVE) uses another approach in their documentation of emission where they consider Norway as a part of the European energy system and by that the exchange of power between neighbour countries. A considerable insecurity with NVE's method is the assumption that all imported energy is produced in the country it is directly imported from, and hence that energy does not cross more than one border[6]. Still, energy will, most likely, cross several borders before being consumed. With this in mind, it is desirable to apply a more detailed method to the energy system to gain information about emission.

A sensitivity analysis will give information about how the power system changes due to alteration in magnitude of source or load, but not about where power from generators actually ends up or from where power to loads actually originates. The Power Flow Tracing (PFT) method, on the other hand, can reveal the origin of energy and hence the amount of GHG emitted due to specific loads[4]. In Norway, such a method could for example improve the knowledge about the impact of offshore electrification to the energy system.

1.2 Contributions

- In this Master's thesis a model based on the PFT method will be developed and used on predefined scenarios. For going forward the PFT method must be investigated and explained.
- The in-house model will be developed in the programming language Python. It will be able to trace power flows, and for the convenience of this thesis it must be compatible with the EMPS model.
- For demonstration of the model scenarios with offshore electrification in Norway will be used. The results from simulations will be used to analyse how the European energy system responds to the electrification of the Norwegian continental shelf (NCS). By finding where the power that is consumed at offshore platforms originates from, the total benefit of electrification, concerning emission, can be determined.

- The model can be useful later for other applications, such as investigation of specific transmission lines or other areas. Since this will be an in-house model it is relevant for internal use and research at the Department of Electric Power Engineering, NTNU.

1.3 Organisation of thesis

The organisation of this thesis is as follows:

Chapter 2: All information and theory which is necessary for understanding this thesis is given. The information includes a description of how the foundation for this thesis was developed by using the EMPS model, and an explanation of electrification of oil- and gas platforms. The theory includes a description of the Power Flow Tracing Method, assumptions done and examples of relevant algorithms.

Chapter 3: The method, which is development of and simulations with a model, is presented. The model gets called the PFT Model and its purpose is to trace the electric power in a power system. Some limitations associated with this model are pointed out, as they can be useful to have in mind when reviewing the results. The scenarios used for simulation are scenarios with offshore electrification in Norway.

Chapter 4: The results from the simulations are presented and explained. These results are given as both yearly average, and seasonal and daily variations. The workability and credibility of the PFT Model are discussed. Also the impacts of the results, concerning relevance and advantageous, are discussed.

Chapter 5: Concluding remarks are given, together with a summary of the results and some proposals for further work.

Chapter 2

Background

2.1 Impact of offshore electrification in Norway

Remark: This chapter presents work done and results obtained in the NTNU specialisation project "Impact of offshore electrification in Norway to greenhouse gas emissions within the European energy system". The project was conducted in the course "Electric Power Engineering and Energy Systems" (TET4520). The following (Chapter 2.1.1 to Chapter 2.1.4) will therefore consist of extensive reproduction/usage of content from this project[7].

2.1.1 Electrification of offshore oil and gas operations

Of the 50.3 million ton CO₂-equivalents emitted in Norway in 2019, oil and gas operations were responsible for 14.0 million ton, or a quarter[5]. With a national goal of reducing emission with over 50 percent by 2030 and 90 percent by 2050[8], it is essential to cut emission in the oil and gas sector. Equinor, Norway's biggest producer of oil and gas, has presented ambitions of contributing to this reduction through more efficient use of energy, digitisation and most importantly; electrification of fields and facilities[9].

The electrification of offshore oil and gas operations is a direct measure for cutting emission. Gas turbines, which is the common source of energy on the platforms, are replaced with power cables connected to the onshore grid or nearby offshore wind power plants. To remove a gas turbine is equivalent to remove a point-of-emission. A reduction of offshore emission is of course dependent on the imported energy being cleaner than the one produced from gas directly at the platforms. The fact that gas is spared on the platforms, and hence burned somewhere else, is an unavoidable and necessary consequence which together with today's climate politics will reduce the overall emission over time[10].

In 2022 the electrification project on the Utsira High Area will be completed, with Johan Sverdrup as the host field. Johan Sverdrup will then send power further to other large fields. At this point there will be a total of eight offshore oil and gas facilities directly connected to the onshore grid. These, together with the associated installed power capacities from shore given in megawatt (MW), are listed in Table 2.1[11][12].

Table 2.1: Transmission capacity from shore in 2022[12].

Field	Power from shore [MW]
Snøhvit/Melkøya	50
Goliat	75
Ormen Lange/Nyhamna	350
Troll	184
Martin Linge	55
Gjøa	40
Utsira High	300
Vallhall	78

2.1.2 The EMPS model

The program used for simulations of the European energy system was EFI¹'s Multi-area Power market Simulator (EMPS, also known as "Samkjøringsmodellen" in Norwegian). This is a program made for long time forecasting and planning of the electricity market, and it is possible to choose different scopes and years for simulations. The scope could for example be only the Nordic countries or Northern Europe. The chosen scope is divided into smaller areas that are electrically connected to each other with power transfer lines of determined capacities. These areas can represent countries or parts of countries, and they hold information about local power production and loads. The year chosen is the average of 75 different climate years, and the average year has a time resolution of 6 hour-mean values, based on the defined period-length in EMPS. The main objective of the program is to minimise the total expected cost, or maximise the total socioeconomic benefit, which resembles the efficient system desired[13].

The model developed and used in the specialisation project was named the EMPS 3 Model, and it is the second expansion of the EMPS 1 Model. The EMPS 1 Model was developed by, amongst others, supervisor Associate Professor Steve Völler[14], while

¹Elektrisitettsforsyningens Forskningsinstitut, now SINTEF Energy Research.

the EMPS 2 Model was developed by the previous master student Marta Ulvensøen in 2019[15]. The EMPS 3 Model, with explanation of elements and expansions done, can be seen in Figure 2.1. Also, the areas in the EMPS 3 Model are listed in Table 2.2.

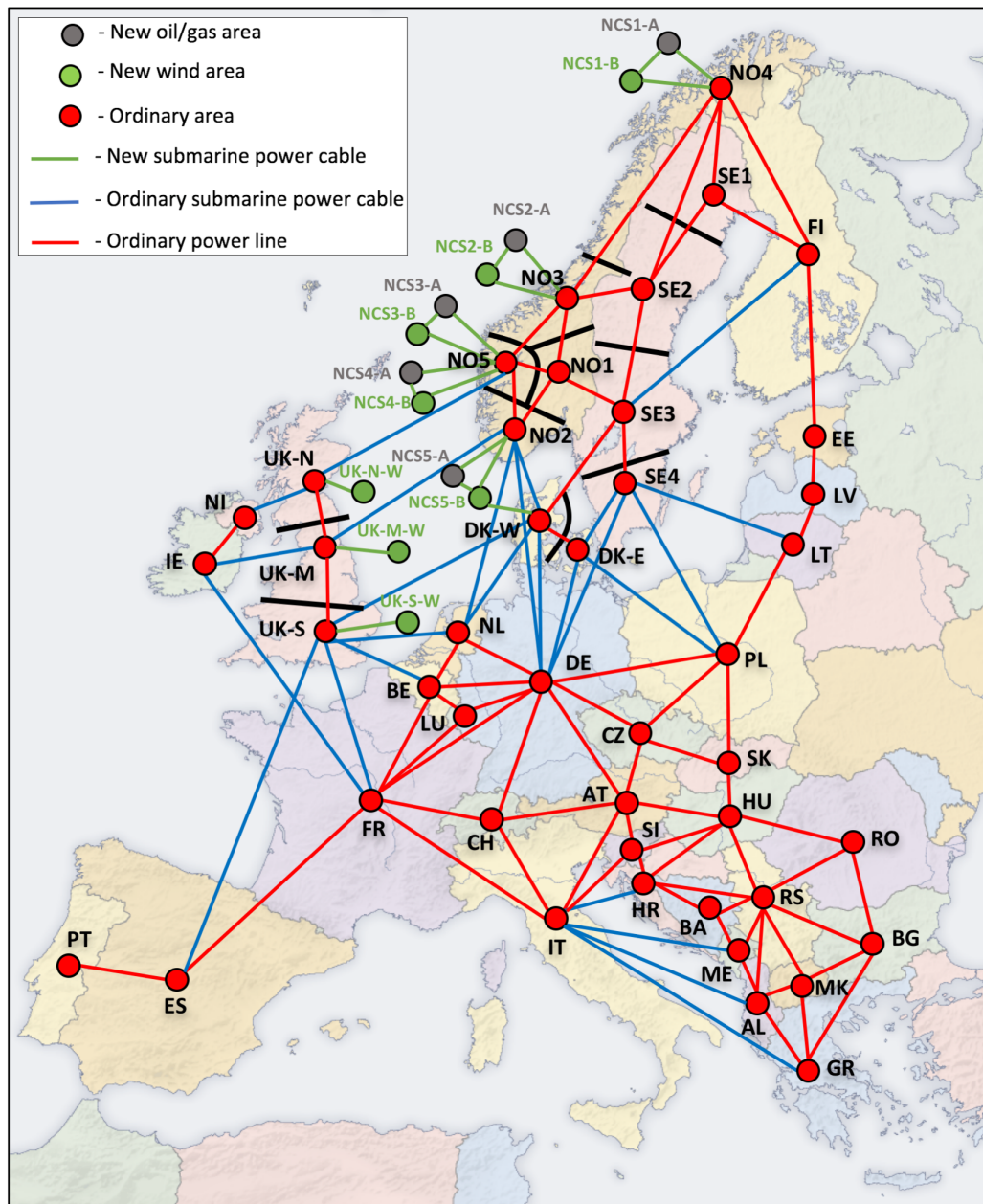


Figure 2.1: The EMPS 3 Model - Model of the European energy system with offshore areas.

Table 2.2: Areas in the EMPS 3 Model.

Area #	EMPS	Name	Area #	EMPS	Name
1	AL	Albania	30	NO4	Norway 4
2	AT	Austria	31	NO5	Norway 5
3	BA	Bosnia and Herzegovina	32	PL	Poland
4	BE	Belgium	33	PT	Portugal
5	BG	Bulgaria	34	RO	Romana
6	CH	Switzerland	35	RS	Serbia
7	CZ	Czech Republic	36	SE1	Sweden 1
8	DE	Germany	37	SE2	Sweden 2
9	DK-E	Denmark East	38	SE3	Sweden 3
10	DK-W	Denmark West	39	SE4	Sweden 4
11	EE	Estonia	40	SI	Slovenia
12	ES	Spain	41	SK	Slovakia
13	FI	Finland	42	UK-N	United Kingdom North
14	FR	France	43	UK-M	United Kingdom Mid
15	GR	Greece	44	UK-S	United Kingdom South
16	HR	Croatia	45	NCS1-A	Norwegian Continental Shelf 1, Oil
17	HU	Hungary	46	NCS1-B	Norwegian Continental Shelf 1, Wind
18	IE	Ireland	47	NCS2-A	Norwegian Continental Shelf 2, Oil
19	IT	Italy	48	NCS2-B	Norwegian Continental Shelf 2, Wind
20	LT	Lithuania	49	NCS3-A	Norwegian Continental Shelf 3, Oil
21	LU	Lucembourg	50	NCS3-B	Norwegian Continental Shelf 3, Wind
22	LV	Latvia	51	NCS4-A	Norwegian Continental Shelf 4, Oil
23	ME	Montenegro	52	NCS4-B	Norwegian Continental Shelf 4, Wind
24	MK	Macedonia	53	NCS5-A	Norwegian Continental Shelf 5, Oil
25	NI	Northern Ireland	54	NCS5-B	Norwegian Continental Shelf 5, Wind
26	NL	Netherland	55	UK-N-W	United Kingdom North, Wind
27	NO1	Norway 1	56	UK-M-W	United Kingdom Mid, Wind
28	NO2	Norway 2	57	UK-S-W	United Kingdom South, Wind
29	NO3	Norway 3			

From the EMPS 2 Model, the EMPS 3 Model has been extended with ten offshore areas in Norway, three offshore areas in UK, and their belonging electric connections. Five of the offshore areas in Norway represents clusters of oil platforms, while the remaining five in Norway and the three offshore areas in UK represents clusters of wind farms. The EMPS 3 Model has a total of 57 areas and 117 transmission lines. Some of these transmission lines, e.g. the one between NO5 and UK-N, are only included in the scenarios in 2045, since they are assumed not yet operating in 2025. The lines associated with the offshore installations in Norway are not included in the base case scenario.

The consumption and installed turbine capacities in the new areas, and the capacities in the corresponding lines, was decided through a literature review in the specialisation project, in order to resemble real life operation and other potential scenarios. Information about consumption and installed capacities on the platforms was collected from a document given by the Norwegian Petroleum Directorate[16], and information about potential offshore wind power projects was collected from a report given by NVE[17]. An overview of the values for consumption and installed capacities can be seen in Appendix A.

2.1.3 Scenarios

In order to model the scenarios, the fossil fuel driven turbines were divided into two categories: mechanical and electrical. The mechanical turbines are the ones used to drive rotating equipment in e.g. compressors directly, while the electrical turbines are the ones used to produce electrical energy for further usage. In the scenarios, the wind turbines were used with installed capacities based on the highest potential presented by NVE. These capacities were either used fully in the scenarios, or were set to zero. The most promising offshore wind power projects were assumed developed by year 2025, while the rest were assumed developed by years 2035 and 2045.

For the specialisation project, it was decided to form three different scenarios: base case scenario, partial electrification scenario and full electrification scenario. The base case scenario was set to year 2025, while the two latter scenarios were set to both years 2025 and 2045. The base case scenario was used to simulate a system without any electrification on the NCS. Offshore wind turbines were only included in UK. In Norway, however, no offshore wind turbines were included and the transfer capacities from land to the platforms were set to zero. Hence, all the offshore power consumption was covered by the installed gas turbines on the platforms.

In the partial electrification scenario offshore wind turbines were included in Norway as well as in the UK. The capacities associated with the aggregated electrical turbines were set to zero, which indicated that parts of the required power needed to be transferred either from the offshore wind turbines or from land, or both. Offshore wind turbines were included in the full electrification scenario as well. Unlike the partial electrification scenario the capacities in both mechanical and electrical turbines were set to zero in the full electrification scenario, indicating that all offshore power consumption had to be transferred from offshore wind turbines or land, or both. An overview of the three different scenarios can be seen in Table 2.3.

Table 2.3: Overview of scenarios.

Installation	Scenario		
	Base case	Partial electrification	Full electrification
Offshore wind (UK)	x	x	x
Offshore wind (Norway)		x	x
Mechanical gas turbines	x	x	
Electrical gas turbines	x		

When simulating the power system over time, it is required to choose one of three power system scenarios for the EMPS. These three are Current Policies (CP) scenario, New Policies (NP) scenario and 450 ppm (450) Scenario. CP, which is the scenario chosen, reflects the world where there is no new policies being implemented. NP reflects a world where prices evolve according to policies and strategies planned by the governments. 450 reflects a world where policies that will keep the global temperature within 2 degrees Celsius above pre-industrial levels in 2100 are implemented[14]. These power system scenarios are based on the report from the World Energy Outlook (WEO) 2016 by IEA[18]. Since these scenarios were modelled in 2020, all of these power system scenarios would probably give approximately the same results in 2025. In 2045, however, a different choice would give different results.

2.1.4 Main results from simulations

Simulating the different scenarios with EMPS resulted in information about active power production mixture in the different areas, given as total gigawatt-hours (GWh) in the chosen year, and active power flow in the lines, given as average MWh for each hour of the year. The information about production mixture was used to find total emission, given

as ton CO₂-equivalents², and CO₂-coefficients for the different areas, given as kilograms of CO₂ emitted from each MWh produced. The total emission, separated into Norway and the rest of Europe, can be seen in Figure 2.2.

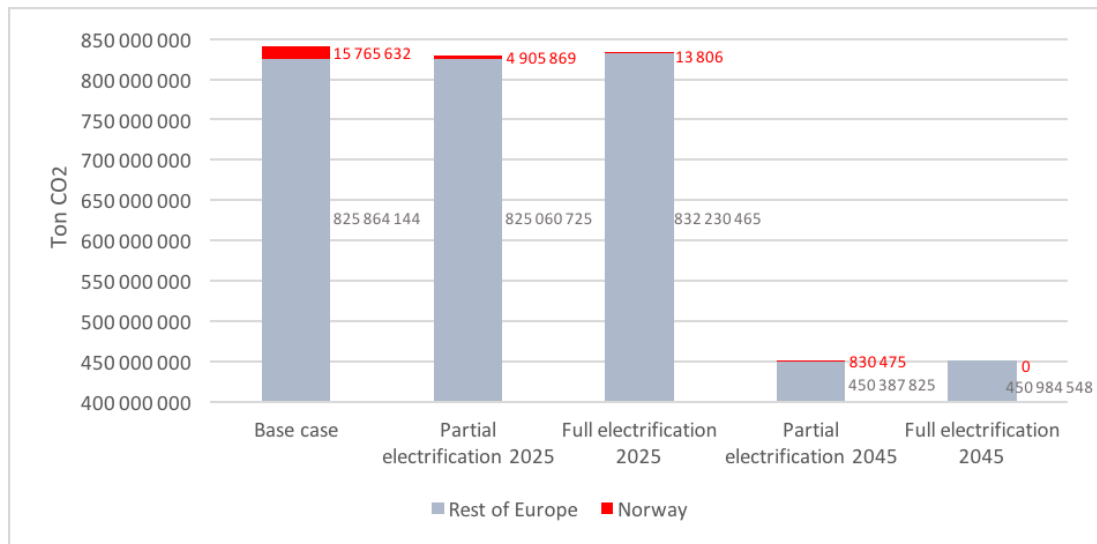


Figure 2.2: Comparison of total emission of CO₂-equivalents in different scenarios.

From Figure 2.2 it becomes clear that the emission will drop significantly over a 20 year period with both partial- and full electrification. This is based on assumptions about future fuel- and CO₂-prices, and future power system developments. The difference between the two scenarios in 2045 is minimal, much because many platforms are assumed retired by then. Still, the full electrification scenario seems to result in less emission. In 2025, on the other hand, the difference between the full- and partial electrification scenario is more substantial, with the partial electrification scenario being the one resulting with least total emission. Both scenarios have less emission compared to the base case scenario.

The reason for that the partial electrification scenario has less emission than the full electrification scenario in 2025 is that the offshore wind energy production, which is present in both scenarios, will not be sufficient to cover the full energy demand on the platforms in 2025. The excess demand in the full electrification in 2025, compared to the partial electrification, is covered by energy produced with coal mainly in Germany, Poland and Finland. The emission from this production is higher than the benefit of uninstalling the offshore mechanical turbines. In 2045 the excess demand will be small

²Equivalents which show how much warming effect the greenhouse gases (Carbon dioxide (CO₂), methane (CH₄), nitrous oxide (N₂O) and fluorinated gases) have, converted to the amount of CO₂[19].

enough to be covered by hydro power produced in Norway and Sweden. The production mix in the different scenarios in 2025, and the difference between these, can be seen in Appendix A. The same information about scenarios in 2045 was included in the specialisation project, but will not be presented in this thesis.

The power flow in the energy system changes when changing scenario, but mostly in 2025. Norway imports electric energy from neighbour countries such as Sweden and Denmark during parts of the year, and mostly in the full electrification scenario. Due to congestion, especially in the lines from Sweden, this power flow will affect the area prices. The power flow in the lines connecting Norway to the rest of Europe, in base case scenario, partial electrification scenario and full electrification scenario, can be seen in Appendix A. For some areas, such as NO3 and NO4, the area prices get affected the same way. This is due to relatively high transfer capacity in the line between the areas. Figure 2.3 shows the price variations over the year for both full- and partial electrification, in three of Norway's five areas. The average price in these areas over the year, also for full- and partial electrification, can be seen in Table 2.4.

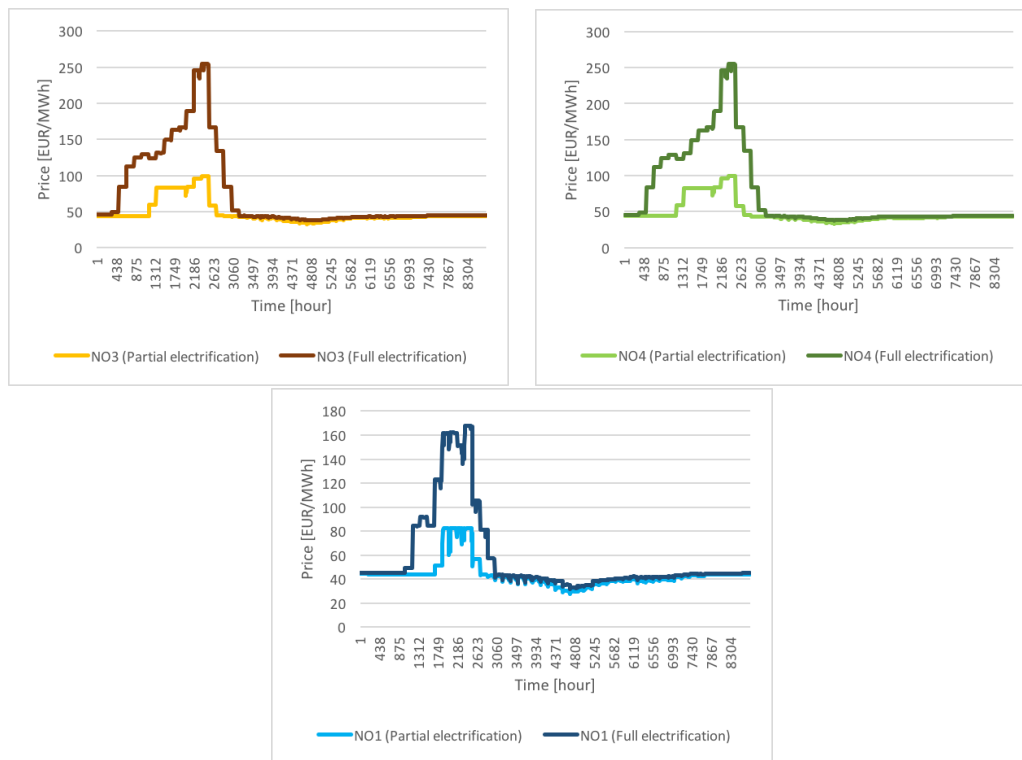


Figure 2.3: Area prices in NO1, NO3 and NO4 for scenarios with partial- and full electrification in 2025.

Table 2.4: Average area prices in Norwegian areas in base case and full electrification in 2025.

Area	Price[EUR/MWh] (Part. el.)	Price[EUR/MWh] (Full el.)
NO1	44.04	57.47
NO3	48.38	74.27
NO4	48.22	74.10

It can be seen in Figure 2.3 that the bottlenecks in the lines which import power to the Norwegian areas appears around hour number 2000 in the year, or March/April. It can also be seen, both in Figure 2.3 and Table 2.4, that there are highest area prices in the full electrification scenario, due to more import and therefore more congestion.

The results from the simulations in the EMPS model form the basis for this thesis. The output from these simulations is in the form of excel files, which will be used as input to the model which will be developed and used in this thesis. Both the power system data and information about emission are of interest.

2.2 Power Flow Tracing (PFT)

It is not possible to physically track electricity from source to load. All energy flows in the same transfer lines which are owned by transmission system operators (TSOs), it is neither practical or feasible to build separate transmission lines for every generation facility. It should be noted that since this makes the distribution of power a natural monopoly, it is strictly regulated[1]. The energy is mixed in the power grid and a consumer cannot separate energy from renewable sources, such as wind and hydro, and fossil sources, such as coal and gas. When power suppliers advertise them self with guaranteed renewable energy, what they actually mean is that one unit of bought and consumed energy corresponds to one unit of electric energy being produced with renewable sources.

Producers of renewable energy holds certificates, called Guarantees of Origin (GOs), which verifies that their energy is clean. The producers sell these GOs to the power suppliers, which lets the power consuming customers "reserve" renewable energy and by that facilitate for clean energy production. However, what origin the actual energy in a specific power socket has, is independent of GOs[20]. This is illustrated in Figure 2.4.

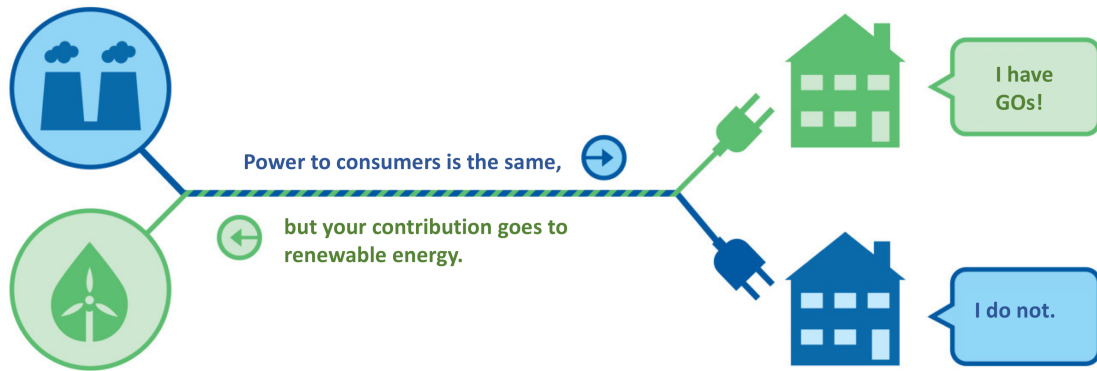


Figure 2.4: Guarantees of Origin[20].

Power Flow Tracing (PFT) is a method that provides theoretical information about contribution of electrical units to the total energy system behaviour and total energy system losses. It makes it possible to correlate power flow in transmission lines to generators and loads, to find the origin of power consumed in a load and to find the receivers of power produced by generators. There exists a range of ways to exploit PFT. Examples of this are environmental studies with CO₂ emission apportioning, allocation of costs concerning maintenance and system loss, and efficient use of load shedding[21].

The PFT method requires information about power generation, demand, line flows and line losses. For this reason, there is a need for power flow analysis or historical measured values in order to implement PFT on a power system. A conceptual diagram for usage of the PFT method can be seen in Figure 2.5.

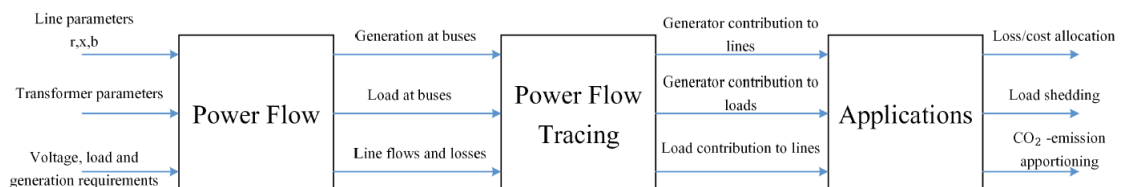


Figure 2.5: Conceptual diagram for usage of the PFT method[22].

In line with the increasing interest for PFT there have been developed various algorithms for estimation of power flow in the system. The recent increased interest is much because of the growing concern about the climate crisis, which gives a desire to both trace emission from source to load and to use the produced energy more efficiently. There are different principles used for development of the PFT method, such as graph theory, circuit theory (Z-bus tracing), optimisation approach, relative electrical distance concept, equilateral

bilateral exchange and game theory. The main principle used, however, is proportional sharing principle (PSP)[23], which will be explained.

2.2.1 Proportional Sharing Principle (PSP)

The concept of proportional sharing is that an area, further referred to as node, in a power system works as a perfect mixer. The nodes can have both inflows and outflows of electric power, and they follow Kirchoff's current law (KCL). The law states that total outgoing power equals total incoming power, when including generators and loads. This must be fulfilled in any electric system. With the idea of nodes being perfect mixers, the contribution of each inflow to each outflow is proportional to the share it holds of the total inflow. This principle is applicable to active power flows, reactive power flows and direct current (DC) power flows[23][4]. An advantage of PSP is that it is relatively easy to understand, and by that easy to use when developing and implementing PFT algorithms. PSP is illustrated in Figure 2.6.

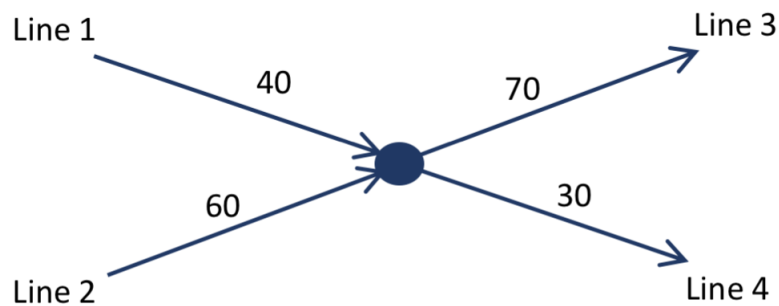


Figure 2.6: Proportional sharing principle[4].

With the total inflow and outflow both being 100, as seen in Figure 2.6, KCL is obtained. There are two inflow branches, Line 1 and Line 2, and two outflow branches, Line 3 and Line 4. According to PSP Line 1 injects:

$$\frac{40}{40 + 60} \cdot 70 = \underline{\underline{28}} \text{ units in line 3}$$

$$\frac{40}{40 + 60} \cdot 30 = \underline{\underline{12}} \text{ units in line 4}$$

And Line 2 injects:

$$\frac{60}{40 + 60} \cdot 70 = \underline{\underline{42}} \text{ units in line 3}$$

$$\frac{60}{40 + 60} \cdot 30 = \underline{\underline{18}} \text{ units in line 4}$$

PSP can neither be proved or disproved, since it is "impossible to 'dye' the incoming flows and check the colour of the outflows". Still, PSP is used with credibility since it generally agrees with common sense[4]. The fact that this assumption of nodes being perfect mixers leads to potential inaccuracy is discussed in Section 3.2.

2.2.2 PFT algorithms using PSP

Amongst the PFT algorithms using PSP are the ones proposed by the English scholars[24] Janusz Bialek in 1996[4] and Daniel Kirschen in 1997[25]. Their algorithms are much used, and the main difference between them is that Bialek's algorithm is node based while Kirschen's algorithm is "common" based. This means that Kirschen's algorithm gives information about generator domains, which are groups of loads supplied by common generators, rather than each individual loads such as Bialek's algorithm does. It is discussed if assuming that a whole "common" gets the same contributions from generators, and that counter-flows within the "commons" are ignored, makes Kirschen's algorithm too simple[26][25].

Another algorithm using PSP is the one presented by Sobhy Abdelkader in 2007. This algorithm is, similar to Bialek's algorithm, node based. Unlike Bialek's algorithm, which has to modify the power system in order to handle losses, does Abdelkader's algorithm handle losses directly[27]. Since Bialek's algorithm is the one chosen for implementation in this thesis, it is the only one which will be explained further. How and why Bialek's algorithm is chosen will be explained in Section 3.1.2.

2.2.3 Bialek's algorithm

Bialek's algorithm is based on linear equations and it consists of two parts; an upstream-looking algorithm and a downstream-looking algorithm. The algorithm works on lossless systems, but since this normally is not the case for power systems Bialek suggested three ways of altering the system for applying the algorithm. This meant to either use average flow, gross flow or net flow. All three approaches require changes in either loads or generators or both, in addition to the line flows, in order to satisfy KCL. The calculation of contributions is then done on the equivalent network. It should be noted that these alterations of the system leads to inaccuracies in the solution from the algorithm. This will be discussed in Section 3.2.

Tracing electricity using average line flow is done by using the average flow in the lines and modifying power injections on both ends of the lines to create the equivalent net-

work. With KCL fulfilled after the modifications contributions from generators and loads to the system can be calculated. Average line flow can be used for both upstream- and downstream-looking algorithm.

Tracing electricity using gross flow is done by using the actual values for power generation at nodes and assuming that no power is lost in the system. The generation stays the same as for the actual network throughout the algorithm, while the loads are increased to hold both their actual values and an allocated part of the loss. In order to fulfil KCL the line flows will be changed in the algorithm, making them similar to or higher than the actual sending end flow. After this the new equivalent network can be used to calculate contributions from generators to lines and loads to in system. Gross flow is used in the upstream-looking algorithm.

Tracing electricity using net flow is done by using the actual values for load demand and assuming that the power loss is removed from the line flows. The load stays the same as for the actual network throughout the algorithm, while the generation is decreased to the difference between the nodes actual values and an allocated part of the loss. In order to fulfil KCL the line flows will be changed in the algorithm, making them similar to or lower than the actual receiving end flow. After this the new equivalent network can be used to calculate contributions from loads to lines and generators in system. Net flow is used in the downstream-looking algorithm.

The upstream-looking algorithm looks at the inflows to nodes and gives the contribution from generators to loads and lines in the system. The downstream-looking algorithm looks at the outflows from nodes and gives the contribution from loads to generators and lines. Both algorithms use topological distribution factors, which is where the assumption about proportional sharing comes to use. Bialek's PFT algorithm can be used for active power flow, reactive power flow and DC power flow. For using it on reactive power flow some more alterations to the equivalent network must be made, since the line loss of reactive power in transmission lines usually is too considerable for the assumptions done. Such alterations will not be discussed further, as only active power will be considered. Following the two algorithms, and the methods for allocating losses, will be presented[4][28].

Upstream-looking algorithm using gross flow

The upstream-looking algorithm uses gross line flows and the generation stay the same as for the actual system. The loads and line flows need to change from the actual values, becoming gross loads and gross line flows. The gross loads will be the sum of the actual demand and the allocated part of the loss. In the algorithm nodal through-flows, which are the sum of either inflows to or outflows from nodes, are defined first. Here defined as gross nodal through-flow.

The total gross nodal through-flow of node i , when looking at inflows, is expressed as:

$$P_i^{\text{gross}} = \sum_{j \in \alpha_i^u} |P_{i-j}^{\text{gross}}| + P_{Gi} \quad \text{for } i= 1,2,\dots,n \quad (2.1)$$

where:

- P_i^{gross} is the gross nodal through-flow of node i ,
- α_i^u is the set of nodes directly supplying node i with power (meaning that the relevant lines must be connected to node i and that power must flow towards node i),
- P_{i-j}^{gross} is the gross line flow in line i - j ,
- P_{Gi} in the generation at node i ,
- n is the number of nodes in the system.

It should be noted that since the algorithm is applied to a lossless system will $|P_{i-j}^{\text{gross}}| = |P_{j-i}^{\text{gross}}|$. c_{ji}^{gross} gives the share a gross line flow in line j - i holds of the total gross nodal through-flow in node j , and it can be mathematically written as:

$$c_{ji}^{\text{gross}} = \frac{|P_{j-i}^{\text{gross}}|}{P_j^{\text{gross}}} \quad (2.2)$$

Combining equation 2.1 and 2.2 gives:

$$P_i^{\text{gross}} - \sum_{j \in \alpha_i^u} c_{ji}^{\text{gross}} P_j^{\text{gross}} = P_{Gi} \quad (2.3)$$

which can be written on vector form as:

$$\mathbf{A}_u \mathbf{P}^{\text{gross}} = \mathbf{P}_G \quad (2.4)$$

where:

- \mathbf{A}_u is the upstream distribution matrix,
- $\mathbf{P}^{\text{gross}}$ is the vector of gross nodal through-flows,
- \mathbf{P}_G is the vector of nodal generation.

By assuming that the transmission losses normally are so small that $\frac{|P_{j-i}^{\text{gross}}|}{P_j^{\text{gross}}} \approx \frac{|P_{j-i}|}{P_j}$, the (i,j)-the element of matrix \mathbf{A}_u , $A_{u_{ij}}$, can be found as:

$$A_{u_{ij}} = \begin{cases} 1, & \text{for } i=j \\ -c_{ji} = -\frac{|P_{j-i}|}{P_j}, & \text{for } j \in \alpha_i^u \\ 0 & \text{otherwise} \end{cases} \quad (2.5)$$

where:

- P_{j-i} is the actual flow from node j in line j-i,
- P_j is the actual nodal through-flow of node j.

Using actual line flows and actual nodal through-flows as approximations for the gross line flows and gross nodal through-flows in equation 2.5 is also in line with the assumption of proportional sharing. With equation 2.4 and 2.5 the gross nodal through-flow can be found as:

$$P_i^{\text{gross}} = \sum_{k=1}^n [A_u^{-1}]_{ik} P_{Gk} \quad \text{for } i=1,2,\dots,n \quad (2.6)$$

Equation 2.6 shows the contribution from all system generators k to the gross nodal through-flow of node i, and it can further be used to find the gross line flows, with Equation 2.7, and gross loads, with Equation 2.8. The same approximation for line flows and nodal through-flows, used in Equation 2.5, is used in Equation 2.7. In Equation 2.8 gross load is approximated as the actual load with the same argumentation, such that $\frac{|P_{Li}^{\text{gross}}|}{P_i^{\text{gross}}} \approx \frac{|P_{Li}|}{P_i}$.

$$|P_{i-j}^{\text{gross}}| = \frac{|P_{i-j}^{\text{gross}}|}{P_i^{\text{gross}}} P_i^{\text{gross}} \approx \frac{|P_{i-j}|}{P_i} \sum_{k=1}^n [A_u^{-1}]_{ik} P_{Gk} \quad \text{for all } j \in \alpha_i^d \quad (2.7)$$

where:

- α_i^d is the set of nodes directly supplied with power from node i (meaning that the relevant lines must be connected to node j and that power must flow from node i).

$$P_{Li}^{\text{gross}} = \frac{P_{Li}^{\text{gross}}}{P_i^{\text{gross}}} P_i^{\text{gross}} \approx \frac{P_{Li}}{P_i} \sum_{k=1}^n [A_u^{-1}]_{ik} P_{Gk} \quad (2.8)$$

where:

- P_{Li}^{gross} is the gross load demand at node i,
- P_{Li} in the actual load demand at node i.

Downstream-looking algorithm using net flow

The downstream-looking algorithm uses net line flows and the demands stay the same as for the actual system. The generations and line flows need to change from the actual values, becoming net generations and net line flows. The net generations will be the difference between the actual generation and the allocated part of the loss. In the algorithm nodal through-flows, which are the sum of either inflows to or outflows from nodes, are defined first. Here defined as net nodal through-flow.

The total net nodal through-flow of node i , when looking at outflows, is expressed as:

$$P_i^{\text{net}} = \sum_{j \in \alpha_i^d} |P_{i-j}^{\text{net}}| + P_{Li} \quad \text{for } i=1,2,\dots,n \quad (2.9)$$

where:

- P_i^{net} is the net nodal through-flow of node i ,
- P_{i-j}^{net} is the net line flow in line i - j .

The share that net line flow in line j - i holds of the total net nodal through-flow in node j is:

$$c_{ji}^{\text{net}} = \frac{|P_{j-i}^{\text{net}}|}{P_j^{\text{net}}} \quad (2.10)$$

The combination of Equation 2.9 and Equation 2.10, and the fact that $|P_{i-j}^{\text{gross}}| = |P_{j-i}^{\text{gross}}|$, gives:

$$P_i^{\text{net}} - \sum_{j \in \alpha_i^d} c_{ji}^{\text{net}} P_j^{\text{net}} = P_{Li} \quad (2.11)$$

Which on vector form is:

$$\mathbf{A}_d \mathbf{P}^{\text{net}} = \mathbf{P}_L \quad (2.12)$$

where:

- \mathbf{A}_d is the downstream distribution matrix,
- \mathbf{P}^{net} is the vector of net nodal through-flows,
- \mathbf{P}_L is the vector of nodal demands.

Similar to the upstream-looking algorithm also these flows can be approximated with the actual flows since the transmission losses can be assumed to be low. Hence, $\frac{|P_{j-i}^{\text{net}}|}{P_j^{\text{net}}} \approx \frac{|P_{j-i}|}{P_j}$.

This makes the (i,j)-the element of matrix \mathbf{A}_d , $A_{d_{ij}}$, to be found as:

$$A_{d_{ij}} = \begin{cases} 1, & \text{for } i=j \\ -c_{ji} = -\frac{|P_{j-i}|}{P_j}, & \text{for } j \in \alpha_i^d \\ 0 & \text{otherwise} \end{cases} \quad (2.13)$$

Further, with Equation 2.12 and Equation 2.13, the net nodal through-flow can be found as:

$$P_i^{\text{net}} = \sum_{k=1}^n [A_d^{-1}]_{ik} P_{Lk} \quad \text{for } i= 1,2,\dots,n \quad (2.14)$$

Equation 2.14 shows the contribution from all system loads k to the net nodal through-flow of node i, or how the net nodal through-flow of node i is distributed between the system loads k, depending on if generators or loads are considered as contributors. Equation 2.14 can further be used to find the net line flows, with Equation 2.15, and the net generations, with Equation 2.16. Similar to the approximation of gross load, net generation in Equation 2.16 is approximated as the actual generation.

$$|P_{i-j}^{\text{net}}| = \frac{|P_{i-j}^{\text{net}}|}{P_i^{\text{net}}} P_i^{\text{net}} \approx \frac{|P_{i-j}|}{P_i} \sum_{k=1}^n [A_d^{-1}]_{ik} P_{Lk} \quad \text{for all } j \in \alpha_i^u \quad (2.15)$$

$$P_{Gi}^{\text{net}} = \frac{P_{Gi}^{\text{net}}}{P_i^{\text{net}}} P_i^{\text{net}} \approx \frac{P_{Gi}}{P_i} \sum_{k=1}^n [A_d^{-1}]_{ik} P_{Lk} \quad (2.16)$$

Allocation of losses

When developing this algorithm, Bialek suggested two ways of allocating losses: with proportional sharing and with non-proportional sharing[4]. The alternative of proportional sharing uses the consistently used PSP and shares the system loss proportionally between nodes according to their demand/generation, and the flow leading to/from them. The alternative of non-proportional sharing uses the fact that transmission loss is proportional to the squared current ($P = R \cdot I^2$) and tries to allocate the losses thereafter, by modifying the proportional sharing method with an exponent in which the distribution factor is raised. The exponent is typically set between 1 and 2. Following the allocating using proportional sharing will be explained, as this is the one chosen when implementing the algorithm in this thesis.

For the upstream-looking algorithm, the loss is allocated to individual loads as the difference between the gross load and the actual load. The gross load shows what would

be the actual load if the system was completely lossless, and if the network was fed by the same generation as the actual system. The loss that each load, L_i , contributes to the system is given as:

$$\Delta P_{L_i} = P_{L_i}^{\text{gross}} - P_{L_i} \quad (2.17)$$

For the downstream-looking algorithm, the loss is allocated to individual generators as the difference between the actual generation and the net generation. The net generation shows what would be the actual generation if the system was completely lossless, and if the network had the same demand as the actual system. The loss that each generator, G_i , contributes to the system is given as:

$$\Delta P_{G_i} = P_{G_i} - P_{G_i}^{\text{net}} \quad (2.18)$$

For the line loss, it might be intuitive to think that it could be found as the difference between the gross line flow and the actual line flow. However, this difference is higher than the actual line loss. This is because the difference also includes loss from other lines that supplies the applicable line. The transmission loss in line i-j can be given as:

$$\Delta P_{i-j} = |P_{i-j}^{\text{gross}}| - |P_{i-j}| - \Delta P_{i-j}^u \quad (2.19)$$

where:

– ΔP_{i-j}^u is the unknown accumulated upstream line loss, which is passed over from adjacent lines.

Since the loss in the system is the same for the input in both upstream- and downstream-looking algorithm, the sum of allocated loss in loads/generator is the same for both algorithms.

Bialek's way of allocating losses allows individual loads and generators to be charged for the actual amount of power lost, and it is therefore in line with the general desire of an efficiently operated energy system. It will, most likely, be an incentive for building more homes and industries in energy effective places. On the other hand, it will penalise those who for some reason are located in long electrical distance from rest of the power grid. Today, the default method of allocation losses is the postage stamp method, or pro rata. The postage stamp method allocates losses only based on the amount of transacted energy, not the electrical distance it has to travel[29]. The different ways of allocating loss will be further discussed in Section 4.4.3.

Chapter 3

Applied Methodological Approach

3.1 Development of the Power Flow Tracing (PFT) Model

3.1.1 Input to the model

There is generally, as mentioned in Section 2.2, need for a power flow analysis or historical measured values to implement the PFT method. In this thesis, however, the required system values will be provided by simulations with the EMPS 3 Model (described in Section 2.1.2). Hence, the input files to the Power Flow Tracing Model (PFT Model) are files from the EMPS 3 Model, or other files with similar setup.

In order to use Bialek's algorithm on data from EMPS, local handling of power demand will be assumed. This means that each node either has power surplus and operates as a generator or has power deficit and operates as a load, depending on the relation between local power production and consumption. This assumption results in that implementation of the PFT method only requires line flows and losses, since the generations and demands are found by the difference in power flowing from and power flowing to the areas. The file which is made from the EMPS simulations that show the power flow in each line each hour throughout a year, given in MWh/h, is called "UTV_hours_AVG.csv". The file which is listing the percentages for loss and transfer capacities in lines is called "maskenett.csv". "maskenett.csv" is not an output from the EMPS model, but it is used by the EMPS model and will in this thesis be used for both the tracing and the visualisation.

The approach used in this thesis assumes that the system is already simulated in EMPS and that demands are handled locally. This approach is shown in Figure 3.1.

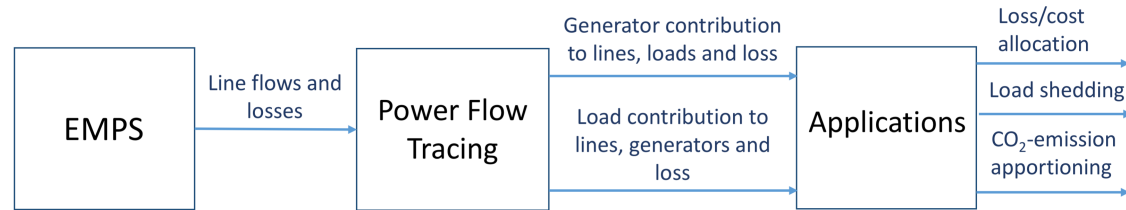


Figure 3.1: Conceptual diagram for usage of the PFT method, starting with EMPS and assuming local handling of loads.

There are no parallel lines in the EMPS 3 model, but if there were the flow in these would have to be combined before execution of PFT. For analysing the results from PFT the file which is giving consumption in the different areas, called "FAST_hours_AVG.csv", will be used together with CO₂-coefficients which have been obtained by combining several of the input/output files to/from the EMPS.

3.1.2 Choosing algorithm

Three algorithms which can be used for performing PFT, and that are based on the PSP, was presented in Section 2.2.2. Since the purpose of this thesis is to look at the nodes within the European energy system individually, are Bialek's algorithm and Abdelkader's algorithm preferable over Kirschen's algorithm. Since Abdelkader's algorithm handles losses directly, it was primarily chosen for further usage.

However, after an attempt to implement Abdelkader's algorithm in Python it was decided to not proceed with it. When applying Abdelkader's algorithm to a small test system it did work as expected, but when applying it to a bigger system (the European system/the EMPS 3 model) some of the result did not make sense. It seemed as if most of the nodes got right values for production, consumption and flow, but that some nodes in mid-Europe (Germany, Switzerland, Austria and Slovenia) had inexplicable values. The reason for this error was not found, but by knowing that also previous master student Kjersti Berg had problems with the exact same algorithm on larger systems[22] it was decided to not pursuit with Abdelkader's algorithm. Bialek's algorithm was instead chosen for further work.

3.1.3 Implementation of algorithm in Python

The PFT Model is developed in the programming language Python and consists of two separate codes. The first code calculates contributions and losses in the power system by using Bialek's algorithm as basis, and will be refereed to as the PFT code. The second

code visualises the results and will be referred to as the Plot code. The model is confidential and can hence only be released for internal use and research at the Department of Electric Power Engineering, NTNU.

The PFT code

The PFT code, which is the one doing the calculations, is implemented by using an approach of five main steps for both the upstream- and downstream-looking algorithm. For the upstream-looking algorithm the steps are:

1. Form the upstream distribution matrix, A_u , with Equation 2.5.
2. Invert A_u , which gives A_u^{-1} .
3. Calculate the contribution from generators to lines with Equation 2.7.
4. Calculate the contribution from generators to loads with Equation 2.8.
5. Calculate the loss allocated to the loads with Equation 2.17.

For the downstream-looking algorithm the steps are:

1. Form the downstream distribution matrix, A_d , with Equation 2.13.
2. Invert A_d , which gives A_d^{-1} .
3. Calculate the contribution from generators to lines with Equation 2.15.
4. Calculate the contribution from generators to loads with Equation 2.16.
5. Calculate the loss allocated to the generators with Equation 2.18.

Before running the code, the three following things must be chosen: algorithm (upstream-looking or downstream-looking), scenario (base case scenario, partial electrification scenario, full electrification scenario or test case) and time frame (hour from and hour to). This will be further used by the code to read the right information from the input folder and perform the power flow tracing. The PFT code does also calculate the average contributions of the time frame.

The output from the PFT code are Excel files which consists of three sheets. The two first sheets are formed as road distance tables, where one gives the contribution from generators/loads to loads/generators, and one gives contributions from generators/loads to lines. The last sheet gives the allocated losses in the loads/generators. These sheets

will be used for further applications and as input for the Plot code. There is one file made for each hour and one file for the average of these hours.

The Plot code

As the input to the PFT Model is the same as the results from the EMPS 3 Model the nodes, or areas, are the same as the ones given in Figure 2.1 and Table 2.2. These areas represent countries, or parts of countries, in Europe. To give a clear presentation of the results from the PFT code, the Plot has code been developed as a map of Europe with lines and nodes which represents the power system. Another code written by Dr. Stefan Jaehnert, Research Manager at SINTEF Energy Research, is actively used in the development of the Plot code. Also, the map coordinates used in the Plot code is retrieved from Jaenerts work. Jaehnert wrote his code as part of a study done by SINTEF Energy Research in the TWENTIES Project[30]. If the input to the PFT Model is from another system than the European energy system, the Plot code would need to be modified in order to visualise the results.

The lines and nodes get coloured according to the results from the PFT code. The results are also used to create two colourmaps, one for the lines and one for the areas, which are presented together with the plot for better visualisation. The area/node in focus is coloured blue. If the area in focus is a generating/surplus area, the other areas will be coloured according to how much power they receive from the area in focus. The lines are coloured according to how much of the sending power from the area in focus that flows through them. If the area in focus is a consuming/deficit area, the other areas will be coloured according to how much power they send to the area in focus. The lines are coloured according to how much of the receiving power to the area in focus that flows through them. Red indicates much power, yellow indicated little power and grey indicates no power. If the transfer capacity in a line is zero is the line not included in the figure. A predefined percentage, typically $>1\%$, decides the limit for how much power the lines and areas must hold in order to be included in the plotted figure.

For plotting with a surplus area in focus the upstream-looking algorithm must have been used in the PFT code. For plotting with a deficit area in focus the downstream-looking algorithm must have been used in the PFT code. Using wrong algorithm will result in that only the area in focus will get the colour blue, the other areas and all lines will stay grey.

For showing different versions of the figure, which is made by the Plot code, France (FR), Italy (IT) and Finland (FI) are chosen as examples in Figure 3.2, Figure 3.3 and Figure 3.4 respectively. Figure 3.2 shows how the power flows on yearly average in the European energy system with France (FR), which is a generating area, as the focus area. The scenario used is the full electrification scenario in 2025.

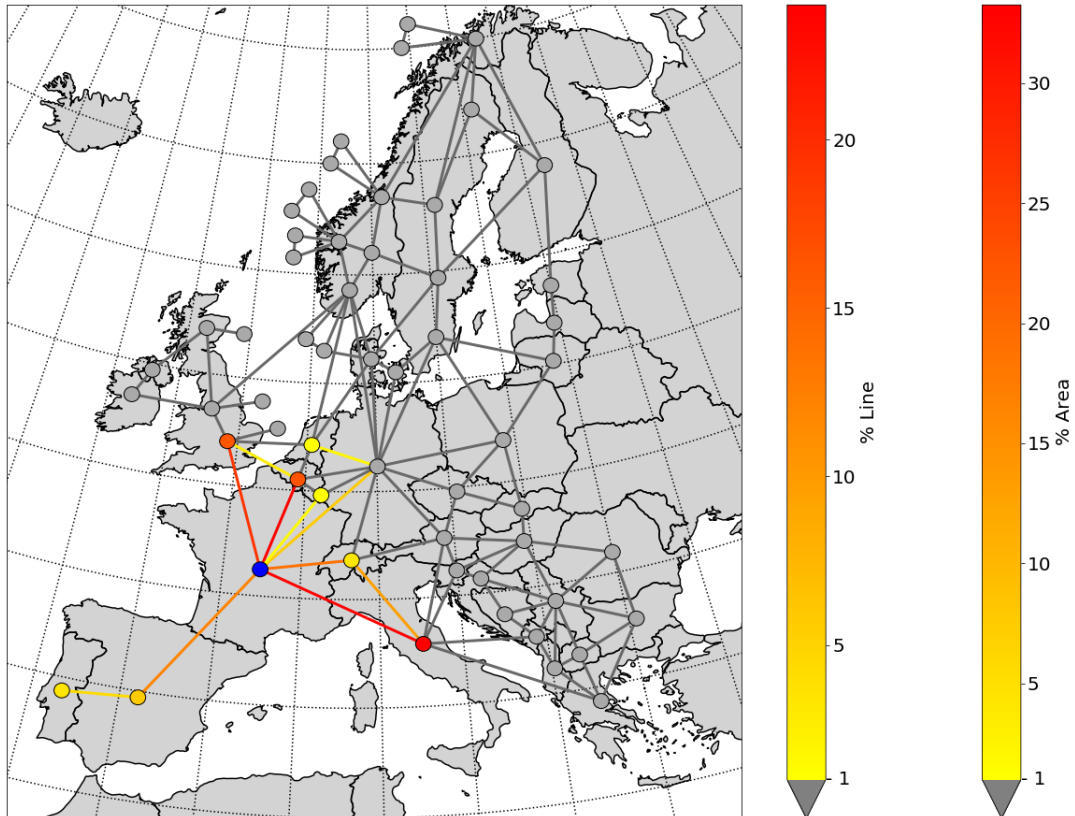


Figure 3.2: Illustration of power flow from France in full electrification scenario, using upstream-looking algorithm.

As seen in Figure 3.2 France sends most of its power (approximately 30%) to Italy, and approximately 10% of this is transferred through Switzerland (CH). Switzerland also consumes some of the power produced in France, but only approximately 5%. Figure 3.3 shows how the power flows on yearly average in the European energy system with Italy, which is a consuming area, as the focus area. The scenario used is the full electrification scenario in 2025.

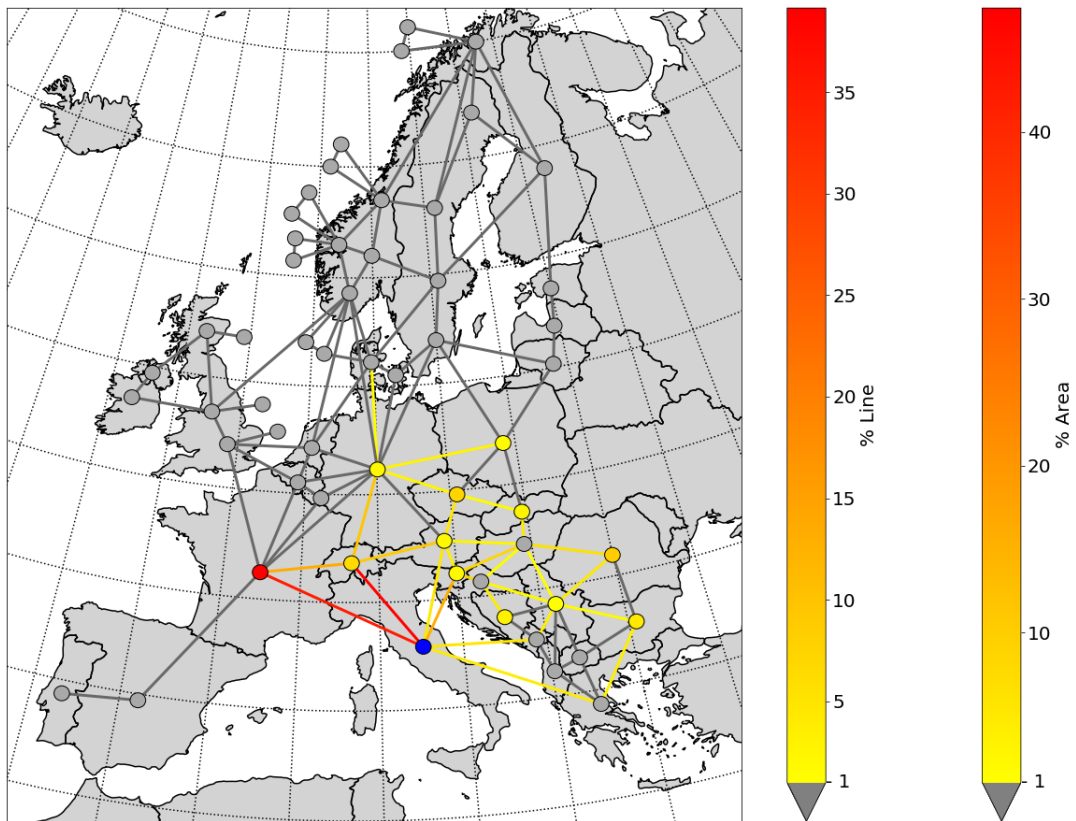


Figure 3.3: Illustration of power flow to Italy in full electrification scenario, using downstream-looking algorithm.

In Figure 3.3 it can be seen that Italy gets most of its power (over 40%) from France, at that this mainly is imported through the lines IT-FR and IT-CH. Figure 3.4 is included to show how the illustration looks when some transfer lines have zero capacity. The scenario used is the base case in 2025, a scenario with no electrification on the NCS and therefore no power cables on the NCS. The area in focus is Finland and the flow is the yearly average.

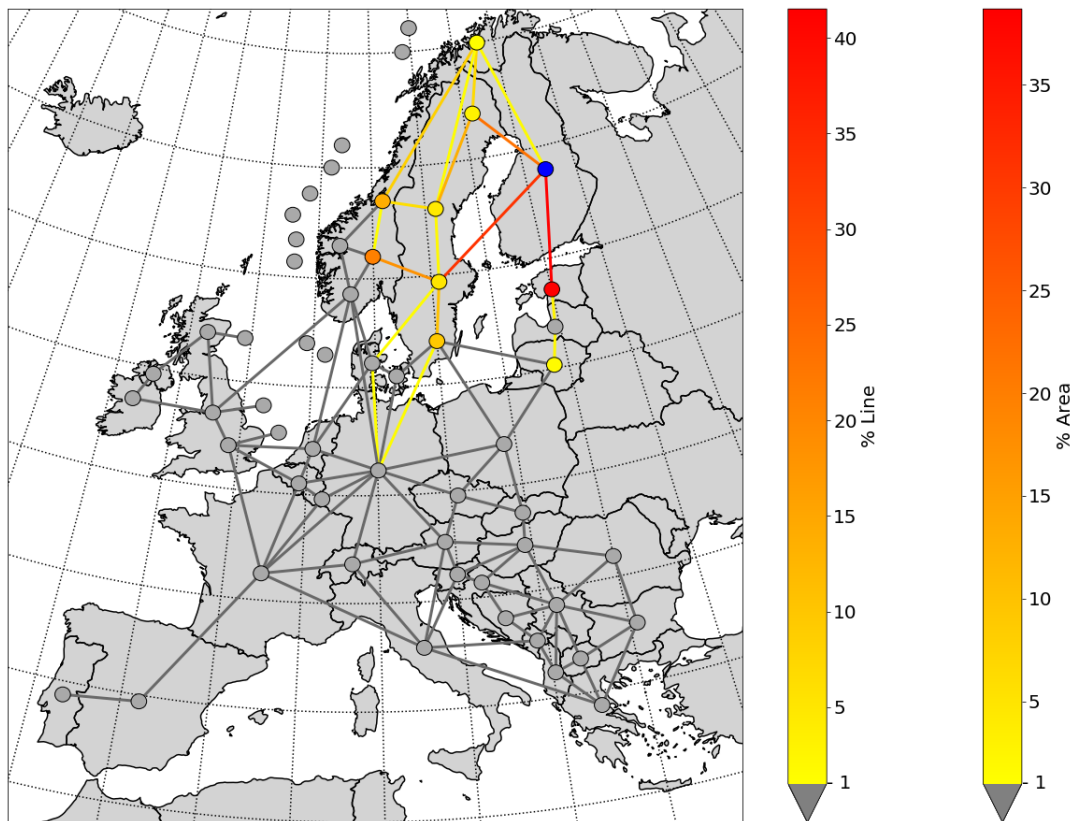


Figure 3.4: Illustration of power flow from Finland in base case, using upstream-looking algorithm.

As seen in Figure 3.2, Figure 3.3 and Figure 3.4 there are two colourmaps to the right of the map, which shows the intensity in the plotted lines and areas. The grey arrow at the bottom of these colourmaps indicates that lines/areas with less power than the chosen percentage, 1% in this case, will get the colour grey.

3.1.4 Verification and validation

In order to give a conclusion based on the output from the PFT Model, the PFT code has first to be verified and validated. This is done in two steps: first by using the PFT code on a smaller system with known behaviour and verifying that the results are correct, and second by analysing the results for different hours of the year to validate that they have consistent and adequate behaviour.

Verification with the Six bus test system

A simple power system with six buses and seven transmission lines, referred to as the Six bus test system, is used for verification of the PFT model. The Six bus test system can be seen in Figure 3.5, and its power system data is collected from another Master's thesis which was written by Kjersti Berg in 2017[22]. The upstream-looking algorithm with gross flow is chosen for comparisons for the verification.

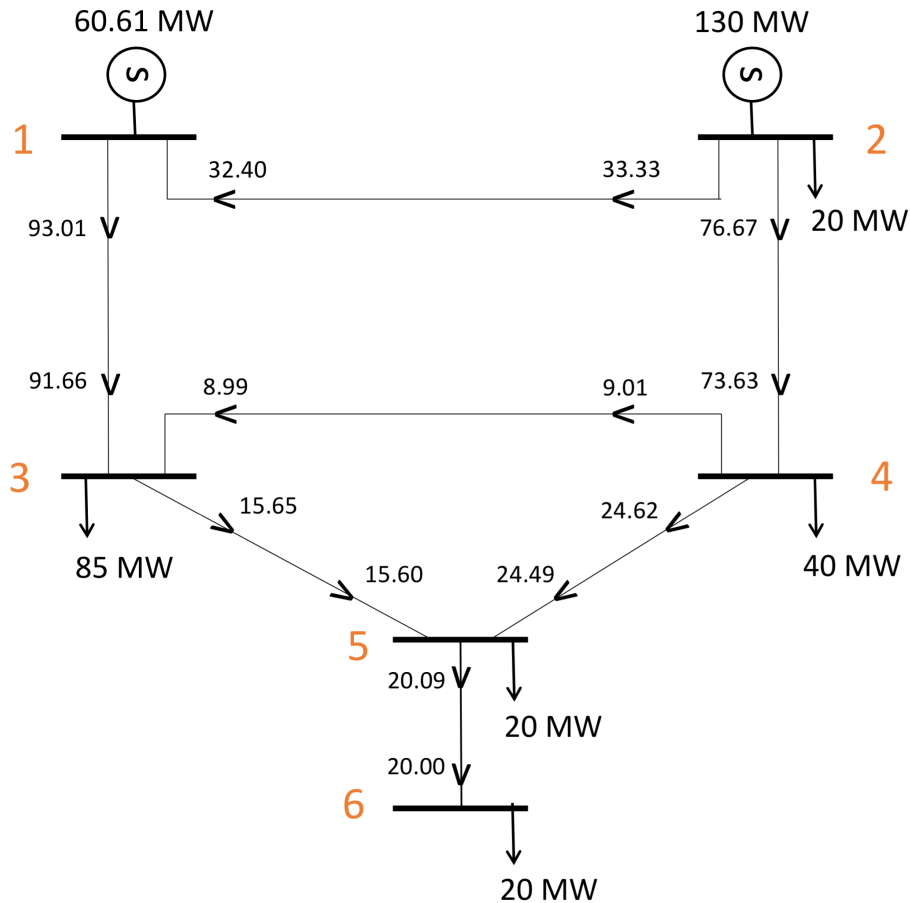


Figure 3.5: Six bus test system[22].

The system has generators at bus 1 and 2. The generator at bus 1 has a capacity of 60.61 MW, and by assuming that loads are handled locally bus 2 has a generator capacity of 110 MW (130 MW-20 MW). The system has loads at bus 3, 4, 5 and 6 with demands of 85 MW, 40 MW, 20 MW and 20 MW, respectively. These magnitudes can be found by adding together the incoming and outgoing power flows, with incoming being negative and outgoing being positive.

First, A_u is found by using Equation 2.5, and when rounded down to three decimals it becomes:

$$A_u = \begin{bmatrix} 1 & -0.303 & 0 & 0 & 0 & 0 \\ 0 & 1 & 0 & 0 & 0 & 0 \\ -1 & 0 & 1 & -0.122 & 0 & 0 \\ 0 & -0.697 & 0 & 1 & 0 & 0 \\ 0 & 0 & -0.155 & -0.334 & 1 & 0 \\ 0 & 0 & 0 & 0 & -0.501 & 1 \end{bmatrix}$$

Second, the inverse of A_u is found. Rounded down to three decimals it is:

$$A_u^{-1} = \begin{bmatrix} 1 & 0.303 & 0 & 0 & 0 & 0 \\ 0 & 1 & 0 & 0 & 0 & 0 \\ 1 & 0.388 & 1 & 0.122 & 0 & 0 \\ 0 & 0.697 & 0 & 1 & 0 & 0 \\ 0.155 & 0.293 & 0.155 & 0.353 & 1 & 0 \\ 0.078 & 0.147 & 0.078 & 0.177 & 0.501 & 1 \end{bmatrix}$$

Third, the contributions to lines from the generators are found using Equation 2.7. The calculations are done for both generators (G1 and G2) and all seven lines (1-2, 1-3, 2-4, 3-4, 3-5, 4-5 and 5-6). For the calculations, all available decimals have been used and the answers have been rounded up to two decimals. The calculations for $P_{G1,1-3}$ and $P_{G2,1-2}$ are shown as example, and all results can be seen in Table 3.1.

$$P_{G1,1-3}^{gross} \approx \frac{P_{1-3}}{P_1} \cdot [A_u^{-1}]_{11} \cdot P_{G1} = \frac{93.01[MW]}{93.01[MW]} \cdot 1 \cdot 60.61[MW] = \underline{\underline{60.61MW}}$$

$$P_{G2,1-2}^{gross} = -P_{G2,2-1}^{gross} \approx \frac{P_{2-1}}{P_2} \cdot [A_u^{-1}]_{22} \cdot P_{G2} = -\frac{33.33[MW]}{(33.33 + 76.67)[MW]} \cdot 1 \cdot 110[MW]$$

$$= \underline{\underline{-33.33MW}}$$

Fourth, the contributions to loads from the generators are found using Equation 2.8. The calculations are done for both generators (G1 and G2) and all four loads (L3, L4, L5 and L6). Also here all available decimal have been used in the calculations and the answers have been rounded up to two decimals. The calculations for $P_{G1,L3}$ and $P_{G2,L3}$ are shown as example, and all results can be seen in Table 3.1.

$$P_{G1,L3}^{gross} \approx \frac{P_{L3}}{P_3} \cdot [A_u^{-1}]_{31} \cdot P_{G1} = \frac{85[MW]}{(91.66 + 8.99)[MW]} \cdot 1 \cdot 60.61[MW] = \underline{\underline{51.19MW}}$$

$$P_{G2,L3}^{gross} \approx \frac{P_{L3}}{P_3} \cdot [A_u^{-1}]_{32} \cdot P_{G2} = \frac{85[MW]}{(91.66 + 8.99)[MW]} \cdot 0.388 \cdot 110[MW] = \underline{\underline{36.07MW}}$$

Table 3.1: Results from applying the upstream-looking algorithm with gross flow on the Six bus test system.

Generator	Load [MW]				Line [MW]						
	3	4	5	6	1-2	1-3	2-4	3-4	3-5	4-5	5-6
1	51.19	0	4.70	4.72	0	60.61	0	0	9.42	0	4.72
2	36.07	41.66	16.10	16.18	-33.33	33.33	76.67	-9.38	6.64	25.64	16.18

Running the PFT code for the six bus test system gives exactly the same results. This implies that the PFT code is working as intended. In addition the PFT code gives a total allocated loss of 5.61 MW. This magnitude can also be found by adding together generator capacities and load demands in the Six bus test system, with generators as positive and loads as negative. The result files from the PFT code for the Six bus test system can be seen in Appendix B.

Validation with a EMPS 3 Model scenario

The validation approach for the PFT code is done on results from the EMPS 3 Model. The scenario chosen for this is the base case scenario, and both the upstream-looking- and downstream-looking algorithm in the PFT code is validated. To check if the behaviour is consisted for the algorithms four hours of the year are compared. The hours chosen are hours number 1000, 3000, 5000 and 8000. The hours are chosen in such a way that they represents different climate seasons, and by that different power flow patterns, of the year.

The two aspects which are compared are the relation between loss and total flow in the system, and the difference in total system power flow between results from the PFT code and the EMPS 3 Model. The total system loss, which is calculated by the PFT code and given in MW, should be the same for the upstream-looking- and downstream-looking algorithm. Dividing the total system loss with the total system flow from the PFT code gives the relationship between loss and total flow. It should be noted that since the same power flow is sent through several lines, this relation does not correspond to the

total system loss in percent. The relation should be highest for the downstream-looking algorithm, since the downstream-looking algorithm gives flows which are equal or lower than the output of the lines. The upstream-looking algorithm gives flows which are equal or higher than the input of the lines. The system loss and its relation to total flow (given in percentage), for the four different hours, is given in Table 3.2.

For the PFT code to be reliable it is necessary that the difference in total system flow from the PFT code and the EMPS 3 Model is acceptable small and about similar for the different hours. Dividing the calculated difference by the total system flow from the EMPS 3 Model gives the difference in percent. The results from this is also given in Table 3.2.

Table 3.2: Validation of the PFT code using base case.

Hour	System loss in PFT code (left, in MW) and its relation to total flow (right, in %)	
	Upstream-looking algorithm	Downstream-looking algorithm
1000	1428 / 1.63	1428 / 1.69
3000	1204 / 1.57	1204 / 1.63
5000	1202 / 1.58	1202 / 1.63
8000	1341 / 1.63	1341 / 1.70

Hour	Difference in flow between the models (PFT-EMPS 3) (in %)	
	Upstream-looking algorithm (%)	Downstream-looking algorithm (%)
1000	2.52	-0.76
3000	2.64	-1.03
5000	2.56	-0.90
8000	3.00	-1.06

As seen in Table 3.2 the total loss in the system is similar for the upstream-looking- and downstream-looking algorithm, for all hours. This is as expected and implies that the algorithms are implemented correctly. Also, the relation between loss and total flow is higher for the downstream-looking algorithm than for the upstream-looking algorithm, which aligns with the predictions. The difference in the relation between loss and total flow, between the two algorithms, is about the same for all hours (0.05% to 0.07%), which also implies that the code is successful.

The difference in system flow between the two models is, as seen in Figure 3.2, consistent: between 2.5% and 3.0% for the upstream-looking algorithm, and between -0.7%

and -1.1% for the downstream-looking algorithm. They are sufficient small enough for the purpose of this thesis. The reason that the flow from the downstream-looking algorithm in the PFT code is closest to the flow from the EMPS 3 Model, compared to flow from the upstream-looking algorithm, is that the flow in the EMPS 3 Model is given as the output flow of the lines. This is, as mentioned earlier, about the same as for the downstream-looking algorithm. For the upstream-looking algorithm the flow used is similar to or higher than the input flow of the line.

3.2 Limitations in the method

Throughout the development of the PFT Model it has been necessary to make choices and assumptions. Usage of PSP and equivalent power systems are direct consequences of choosing Bialek's algorithm. In order to use the algorithm on the data from EMPS, the assumption of local handling of load had to be made as well. These choices and assumptions must be addressed as potential inaccuracies, and by that limitations, in the results from the PFT Model.

3.2.1 Proportional Sharing Principle

As mentioned in Section 2.2.1 PSP can neither be proved nor disproved, since it is impossible to distinguish power from different sources. There exist several papers trying to prove PSP, but none with any notable results[24]. Still PSP is generally accepted for usage, much because of its hold in common sense. Since PFT is very much based on the assumption of proportional sharing, it must be recognised as an inaccuracy in the PFT Model. Also, since PSP cannot be proven, the result from the PFT Method can neither. If it turns out that power does not mix perfectly, which is the assumption done in PSP, the results from the PFT Model will hold significant errors.

3.2.2 Equivalent power systems

The chosen algorithm, Bialek's Algorithm, works only on lossless systems. Since this is not reflecting real life systems, equivalent systems must be constructed, as explained in Section 2.2.3. This results in that the results, both from the upstream-looking and downstream-looking algorithm, deviates some from actuality. Because of this the results from the PFT Model must be handled thereafter, meaning that it can give indications for how the system reacts rather than precise data. Nevertheless, with the verification and validation done in Section 3.1.4, there is hold in claiming that the results from applying PFT on an equivalent network is valid with acceptable small margins of error.

3.2.3 Local handling of loads

It is assumed that loads are handled locally within the different areas, such that values for generators and loads are merged. This results in that an area, or node, acts either as a generator or a load, never both. This had to be done in order to use the equations in Section 2.2.3, Bialek's algorithm cannot handle nodes as both generators and loads at the same time. For loads to actually be handled locally the generated power in an area would have to be directly transferred to loads within the same area, before being mixed with imported power. Knowing that the power system has continuous flow, it is clear that this assumption is a simplification of the reality, and that it leads to some uncertainty in the results which are made by the PFT model.

3.3 Simulations with the PFT Model

The data base for this Master's thesis, which was presented in Section 2.1, contains system values for three scenarios in both 2025 and 2045. Further, however, only the scenario of full electrification in 2025 will be presented, and in some instances be compared to values from the partial electrification scenario in 2025. Only the figures from the PFT Model, more specific the Plot code, are included. The Excel files that are made by the PFT code, which are further used to make the figures in the Plot code, are not included because they are too big for both the text and the appendix.

The full electrification scenario in 2025 is chosen as main focus because it is the most extreme one considering offshore consumption, and will therefore best show the system trends. All areas on the NCS are simulated, but for the analysis mainly NCS4-A and NCS4-B will be used. The reason for NCS4 being chosen of the five offshore areas on the NCS, is that this is one of the closest ones to other European countries. NCS5 could have been chosen as well, but since this area has relatively much wind power production compared to power consumption, NCS4 was chosen for most realistic results. Simulations of the four remaining offshore areas, with the full electrification scenario, can be found in Appendix C.

In this thesis 1% is chosen as minimum percentage of power in lines and areas that are included in the figure. For values in the night hour number 1 of that day have been used, and for values in the day hour number 12 of that day have been used. Simulations of the night are not presented in this section, but values from them will be included in Section 4.2.

3.3.1 Yearly and hourly flow to offshore installations in Norway

When electrifying the offshore oil- and gas platforms, power will flow towards them from both the nearby offshore wind turbines and other areas in the energy system. Figure 3.6 shows how power in average throughout the year flows towards a group of platforms on the NCS (NCS4-A). Figure 3.7 shows how power flows towards the same area mid-day in the winter (January 1st), while Figure 3.8 shows the same for mid-day in the summer (July 1st). The platforms are consuming areas and therefore the downstream-looking algorithm is used for plotting.

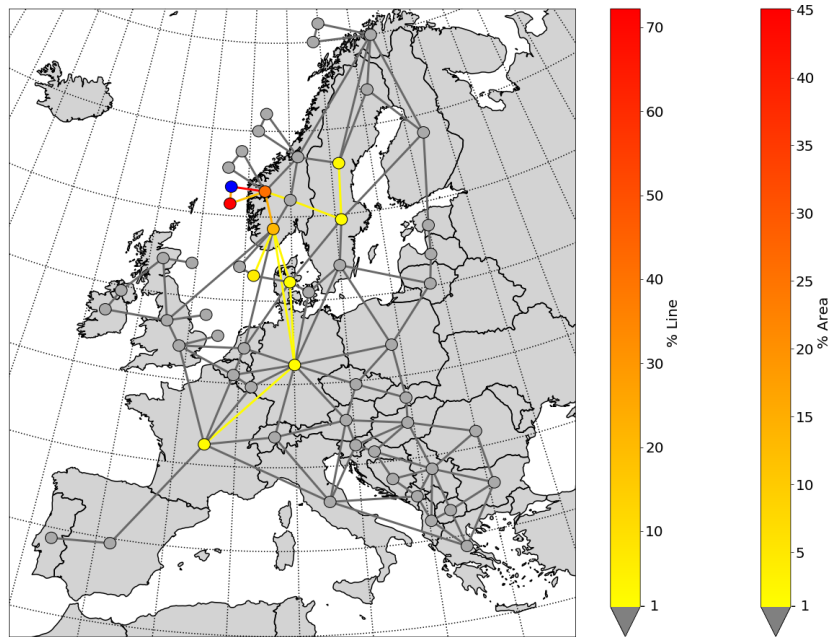


Figure 3.6: Yearly average flow towards NCS4-A.

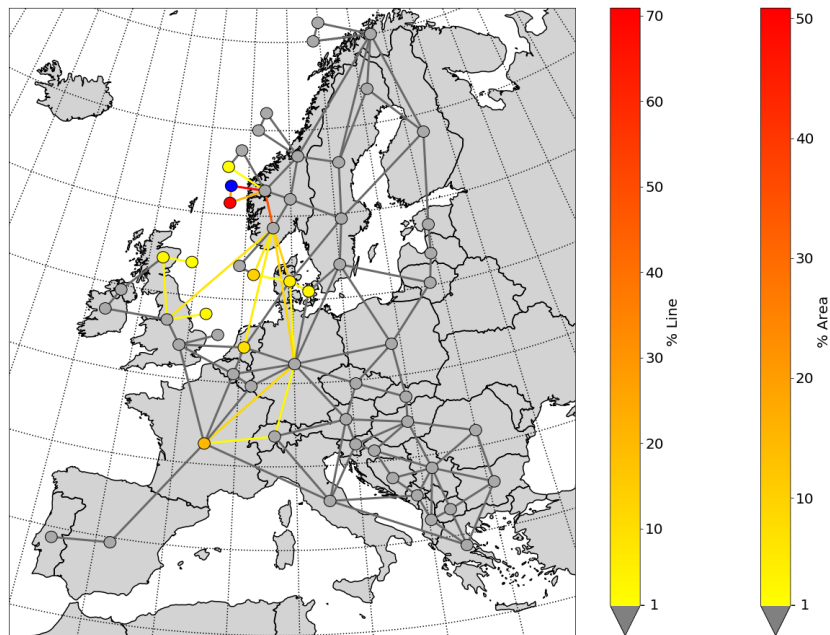


Figure 3.7: Flow towards NCS4-A in the winter.

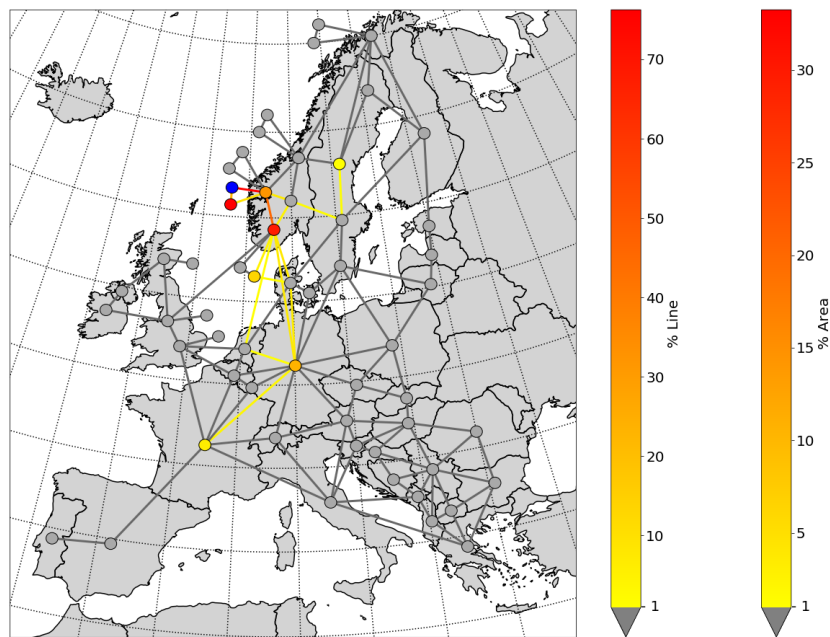


Figure 3.8: Flow towards NCS4-A in the summer.

As seen when comparing Figure 3.7 and Figure 3.8, the power system is acting differently during winter and summer. The yearly average flow towards NCS4-A, seen in Figure 3.6,

resembles most of the flow in the summer. This indicates that the flow towards NCS4-A during rest of the year (spring and autumn) is similar to, or close to, the flow in the summer.

3.3.2 Yearly and hourly flow from offshore installations in Norway

Not all power from the offshore wind turbines is transferred to the offshore platforms. Parts of it flow to other areas of the power system as well. Figure 3.9 shows how power in average throughout the year flows from a group of wind turbines on the NCS (NCS4-B). Figure 3.10 shows how power flows from the same area mid-day in the winter (January 1st), while Figure 3.11 shows the same for mid-day in the summer (July 1st). The wind turbines are generating areas and therefore the upstream-looking algorithm is used for plotting.

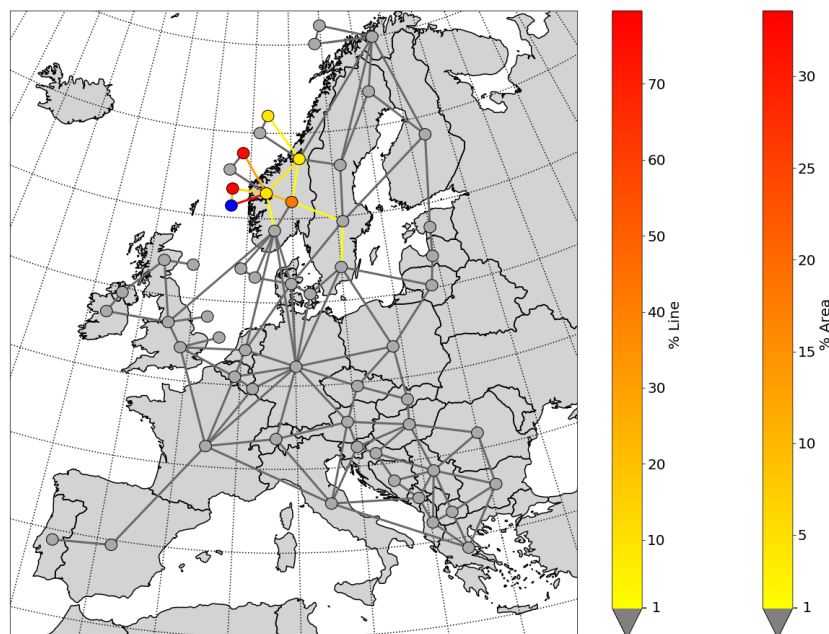


Figure 3.9: Yearly average flow from NCS4-B.

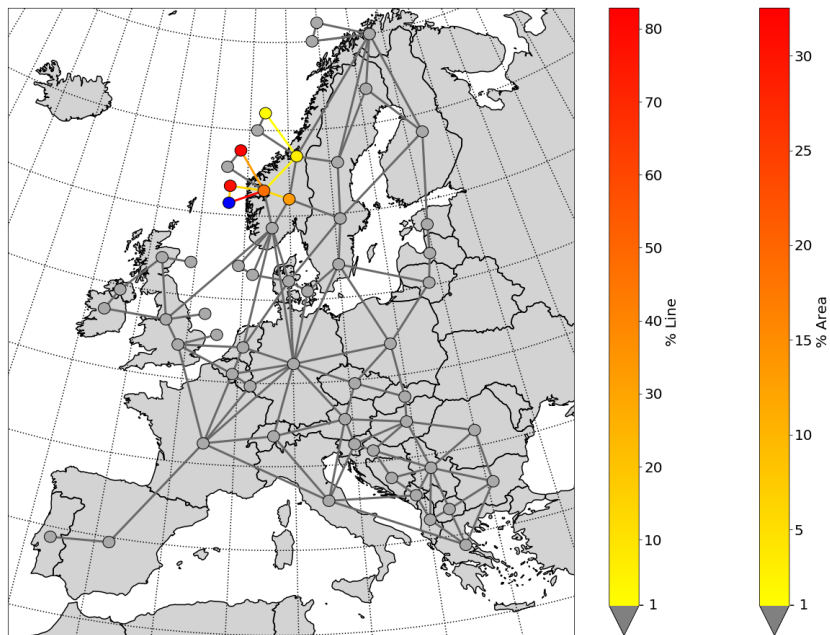


Figure 3.10: Flow from NCS4-B in the winter.

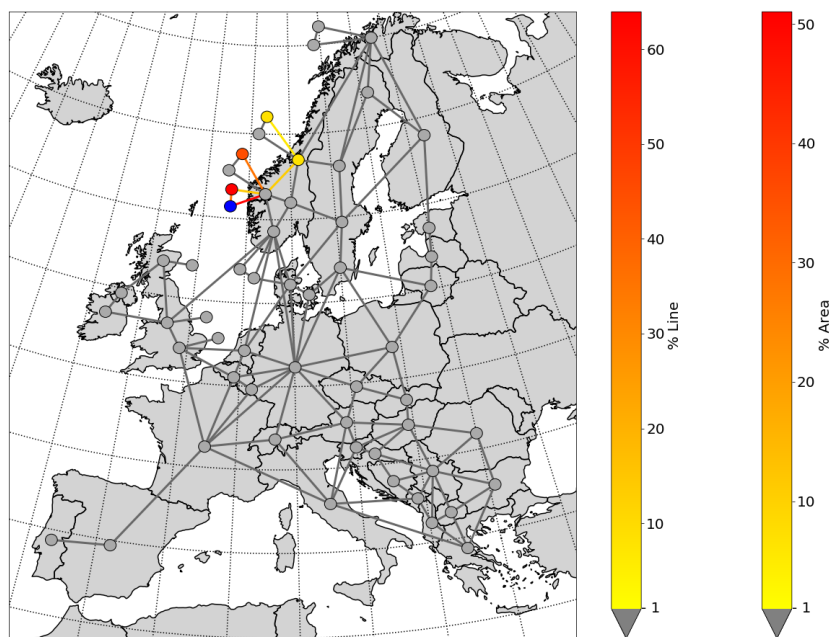


Figure 3.11: Flow from NCS4-B in the summer.

As also seen when comparing Figure 3.10 and Figure 3.11, the power system is acting differently during winter and summer. In the yearly average flow from NCS4-B, seen in

Figure 3.9, are there some more lines (NO1 to SE3, SE3 to SE4, NO5 to NO2) which are relatively more used, compared to both summer and winter. This could be because of different values for demand and production in the energy system during rest of the year.

Chapter 4

Results and Discussion

The result files and figures which are created by the PFT Model can be used to analyse the power flowing to and from areas. The following graphs are made with the Excel files which are obtained from the PFT code.

4.1 Yearly average

To find which areas that import and export most energy the yearly average power flow is used. In this way, presented values gives magnitudes as average energy imported/exported in one hour in 2025. The yearly average CO₂-coefficients for for both the full- and partial electrification scenario can be found in Table D.2 in Appendix D, and will be used to find the emission associated with the imported/exported energy. The coefficients were calculated with data from the specialisation project.

Figure 4.1 shows how much energy each of the offshore areas with oil- and gas platforms import on average throughout the year, in the full electrification scenario. The figure also shows the amount of emission that the imported energy stands for, both as total amount and amount in each GWh. The values have been obtained by using the downstream-looking algorithm, since the areas in focus are consuming areas.

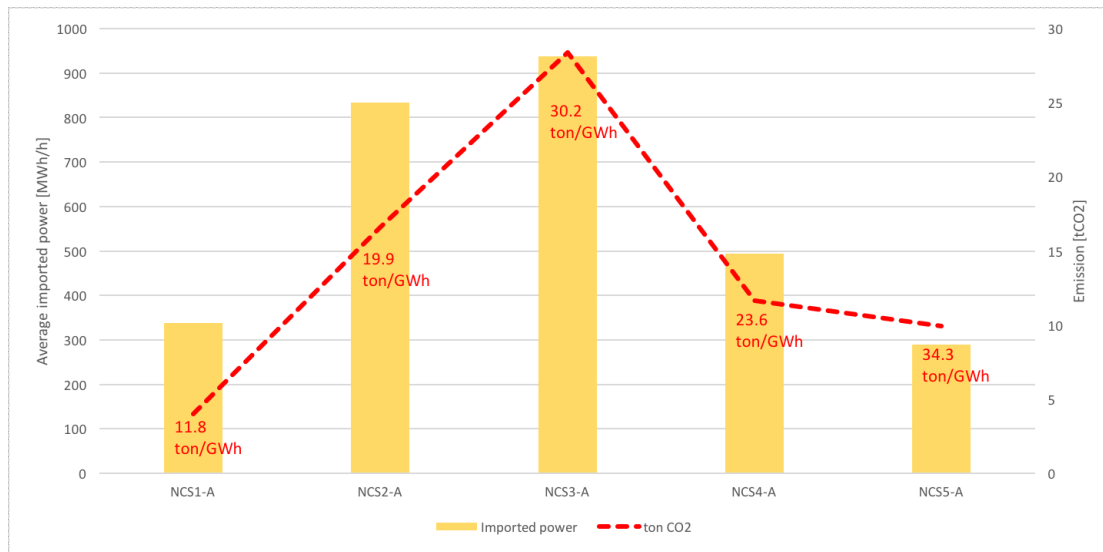


Figure 4.1: Total imported power to platforms on the NCS in the full electrification scenario, obtained by using net flow.

As seen in Figure 4.1 NCS3-A imports most energy, compared to the other areas, while NCS5-A imports the most CO₂-dense energy mix. The fact that NCS3-A imports most energy is align with it being the platform area with most energy consumption in 2025, which can be seen in Table A.1 in Appendix A. The fact that NCS5-A imports the most CO₂-dense energy mix is align with it being the platform area closest to areas in central Europe, which are areas with a less clean energy mix than Norway. With this logic it can be intuitive to think that NCS4-A imports the second highest energy mix, but it is NCS3-A that ranks right under NCS5-A. This is due to the relation between demand and produced power in the associated offshore wind farm. As seen in Figure A.3 in Appendix A, does NCS3-A require much more power than NCS3-B is able to provide. The platforms location can be seen in Figure 2.1.

As explained in Section 2.2.3 the downstream-looking algorithm, which was used when creating Figure 4.1, will trace electricity by using net flow. This results in that the consumed power in the areas is the same in the results as for the actual network. By using upstream-looking algorithm instead the electricity will be traced by using gross flow, and the consumption at loads will increase to hold both their actual values and an allocated part of the loss. In Figure 4.2 the same loads as in Figure 4.1 are presented, but the total consumption, or import, have been obtained by using the upstream-looking algorithm instead. The figure separates the allocated loss from the actual consumed power for better visualisation.

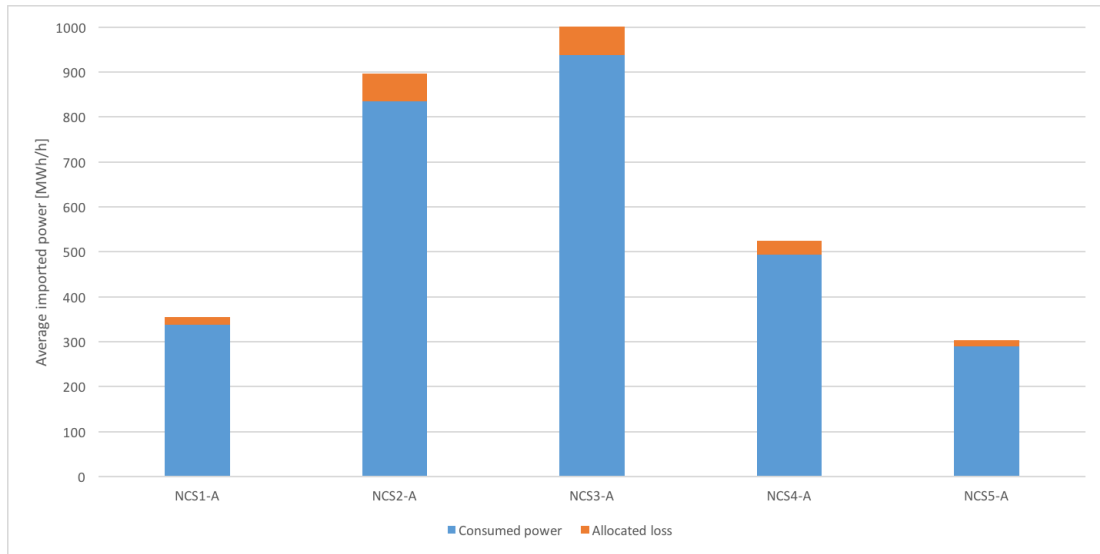


Figure 4.2: Total imported power to platforms on the NCS in the full electrification scenario, obtained by using gross flow.

Comparing Figure 4.1 and Figure 4.2 shows that the value for the loads when using the downstream-looking algorithm is the same as the value for the loads, if not including the allocated loss, when using the upstream-looking algorithm. This is as expected.

When looking closer at NCS4-A the results reveal from which areas the imported energy originates from. This is presented in Figure 4.3, together with the associated emission. The figure is made with values from the downstream-looking algorithm.

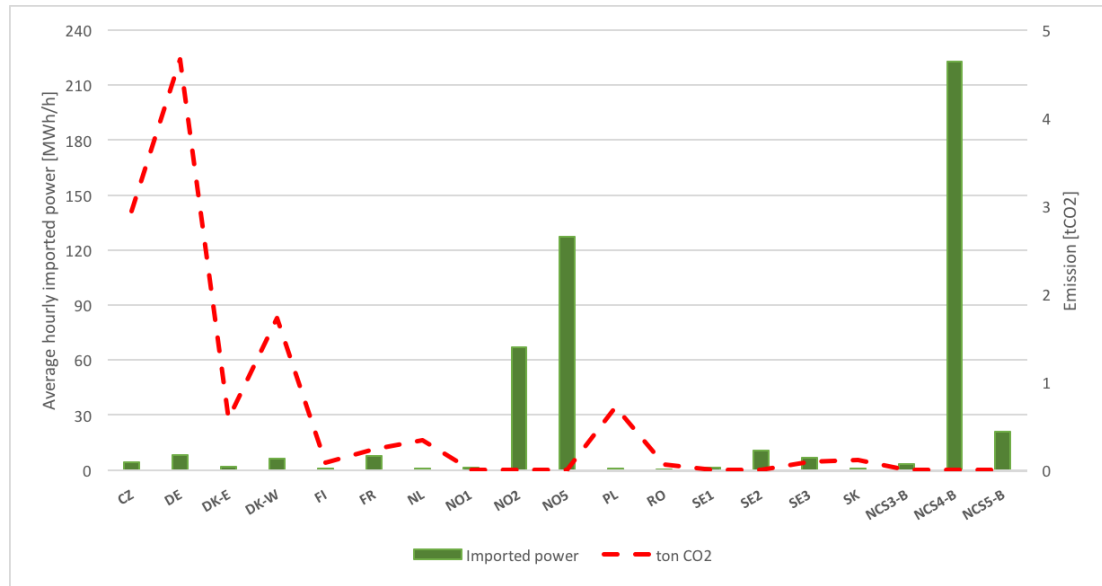


Figure 4.3: Yearly average imported energy to NCS4-A, separated into contributing areas, in the full electrification scenario.

Figure 4.3 shows that most of the power to NCS4-A is imported from the wind power producing area NCS4-B, which lies right next to NCS4-A. This is as expected. Most of the associated emission originates from power production in Germany (DE) and The Czech Republic (CZ), which is because these countries' power production is dominated by power from coal. The production mix in these countries can be seen in Appendix A.

4.1.1 Full electrification versus partial electrification

Comparing the full- and partial electrification scenarios gives information about how the power system responds to changes in magnitude of the offshore electrification. The full electrification scenario requires more imported power than the partial electrification scenario, since the partial electrification scenario says that parts of the demand is covered by local gas power production. The energy consumption in NCS4-A with associated emission for both the full- and partial electrification scenarios can be seen in Figure 4.4.

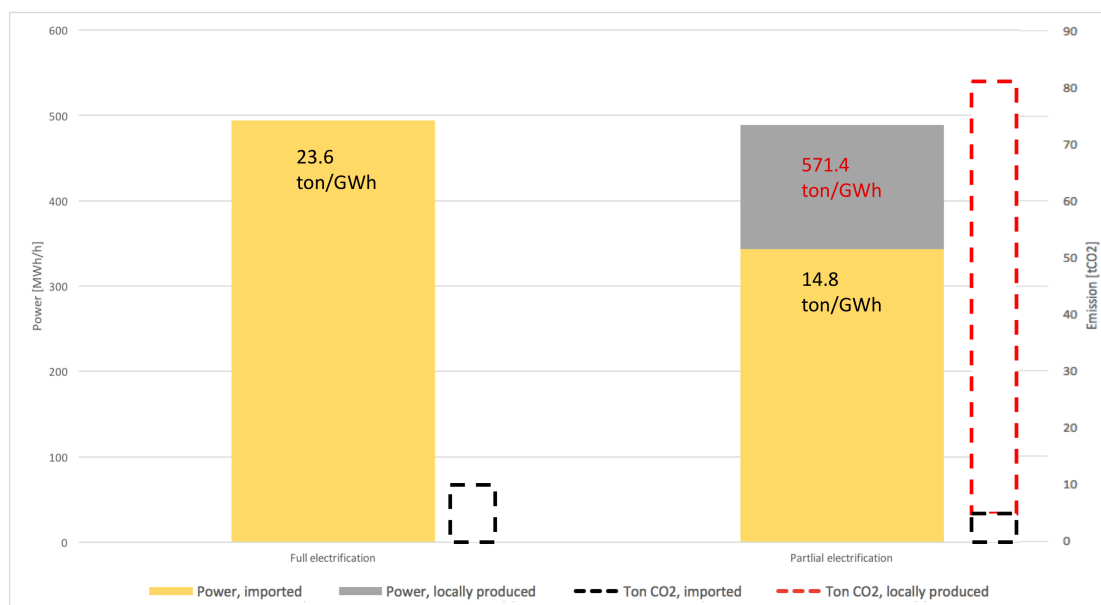


Figure 4.4: Overview of energy consumed, and its associated emission, in NCS4-A for full- and partial electrification.

It can be seen in Figure 4.4 that the total energy consumption is approximately the same for both scenarios. This is as expected, since the production at the plants should be the same. The total associated emission, which is shown to the right of the total consumed energy, is, however, considerable higher for the partial electrification scenario. This is because the CO₂-equivalent of gas, which is 571.4 [ton/GWh]¹ and associated with the local power production at platforms in the partial electrification scenario, is much higher than the CO₂-equivalent of the imported energy to NCS4-A, which is 23.6 [ton/GWh] for the full electrification scenario and 14.8 [ton/GWh] for the partial electrification scenario. Even though the total emission directly linked to NCS4-A is higher for the partial electrification scenario, than for the full electrification scenario, is it important to see this in context with the whole energy system. As discovered in the specialisation project, and shown in Figure 2.2, the partial electrification scenario is overall better concerning emission. This reveals that it exists a limit from where the electrification of oil- and gas platforms actually stops decreasing the GHG, and starts increasing it instead. This also emphasises the importance of having all relevant data when drawing conclusions.

¹The CO₂-equivalent of gas, which emits 0.2 ton CO₂ for each MWh produced[14], in turbines with 35% efficiency. This efficiency was in the specialisation project defined for the electric turbines on the NCS[7].

Since the CO₂-equivalents of the imported energy are different for the different scenarios, it is clear that the imported energy mix is different for the different scenarios. Figure 4.5 shows how the yearly average imported power to NCS4-A changes when going from the partial electrification scenario to the full electrification scenario. The figure is made with the values from Table D.1 in Appendix D, which shows how much each contributing area export to NCS4-A in both the full- and partial electrification scenario, and the difference between the scenarios. Both values for energy and emission are listed.

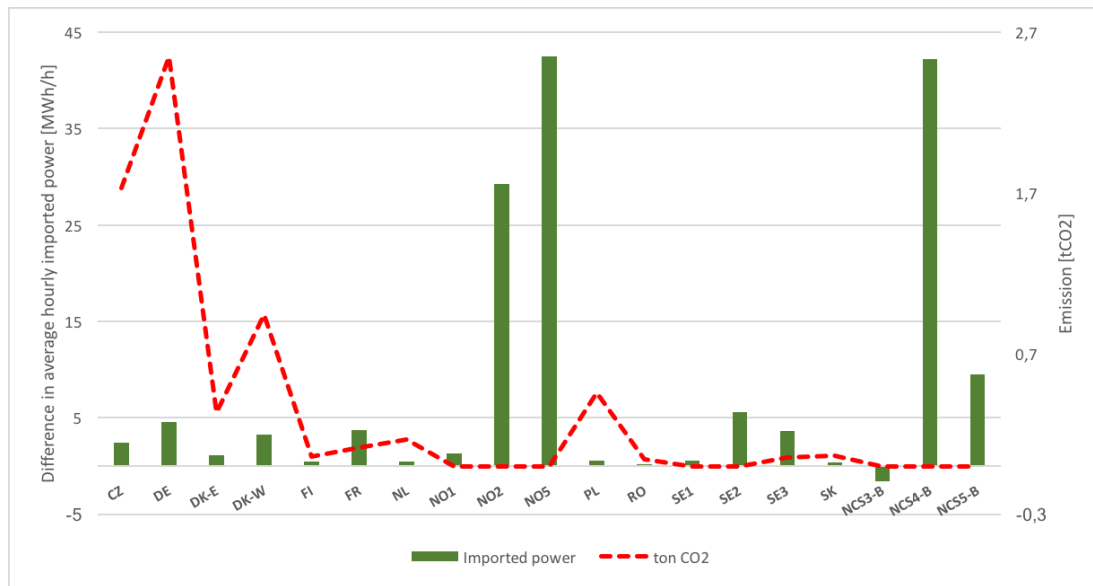


Figure 4.5: Difference between the full- and partial electrification scenarios, in yearly average imported power to NCS4-A, separated into contributing areas.

As seen in Figure 4.5 the areas NO2, NO5, NCS4-B and NCS5-B are the ones that in magnitude gets the highest increase in power exported to NCS4-A, when changing from partial- to full electrification. It is further intuitive to think that these areas export less to other areas in Europe when the scenario shifts, since the consuming areas on the NCS get higher power demands. By using the upstream-looking algorithm the values used for Figure 4.6 have been obtained. The figure shows how the export to different areas from NO2, NO5, NCS4-B and NCS5-B changes when going from partial- to full electrification.

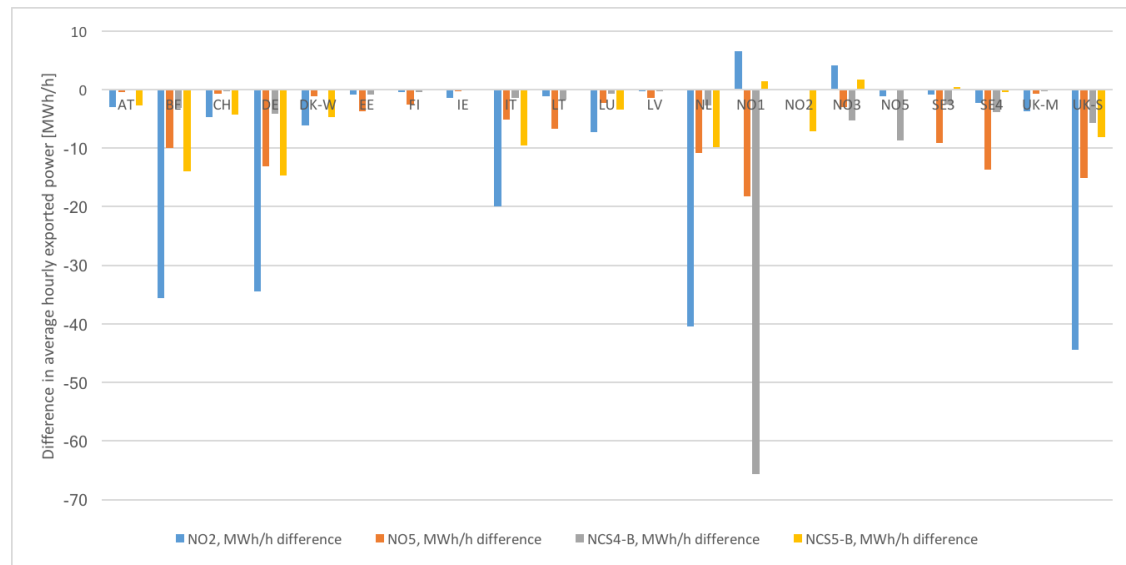


Figure 4.6: Difference in export from areas contributing to NCS4-A, full- vs partial electrification.

From Figure 4.6 it can be seen that NO2 is the area from where the direction of exported energy changes most, from exporting down to areas in central Europe to exporting up to areas on the NCS. NCS4-B exports less to NO1, which again will force NO1 to import its power from other areas in times of high demand. Since Norway is so dominated by hydro power, will a greater electrification hence lead to less export of clean Norwegian hydro power.

4.2 Seasonal and daily variation

For a reminder of where the different areas are situated, see Figure 2.1 again. And to recall, Figure 3.7 and Figure 3.8 show the power flow towards NCS4-A during winter and summer, respectively. Figure 3.10 and 3.11 show the same for flow from NCS4-B. The reason that winter and summer are chosen for investigation of seasonal variations, is that these holds these seasons have different extremes concerning weather, and by that power production and consumption.

When comparing Figure 3.7 and Figure 3.8, it can be seen that more of the imported power in NCS4-A origins from wind in the winter, than in the summer. This is especially clear when looking at the offshore wind power producing areas UK-N-W, UK-M-W and NCS3-B, which only are contributing in the winter. Also DK-W and DK-E, which are areas in the wind power dominated country Denmark, are only contributing in

the winter. In the summer, on the other hand, especially the two areas NO2 and NO5 are contributing considerable more to NCS4-A. These areas are strongly dominated by hydro power. The observations agree with the fact that the wind is strongest in the winter[31], which leads to more wind power production, and that there is more water in the hydro power plant magazines during the summer, which leads to more hydro power production.

The combination of less wind power production and more hydro power production in the summer can also be confirmed when comparing Figure 3.10 and 3.11. With less wind in the summer there are less areas that can receive power from NCS4-B, while at the same time areas with installed hydro power capacity can cover its own demands and do therefore not need import from wind power areas. This does that wind power and hydro power compliments one another.

By graphically visualising the values obtained in the PFT Model the difference between winter (Figure 4.7) and summer (Figure 4.8) can be further analysed. In these figures also the difference between night and day can be seen. Both figures show the imported energy mix in NCS4-A in the full electrification scenario. For these figures the downstream-looking algorithm have been used since there is a consuming area in focus.

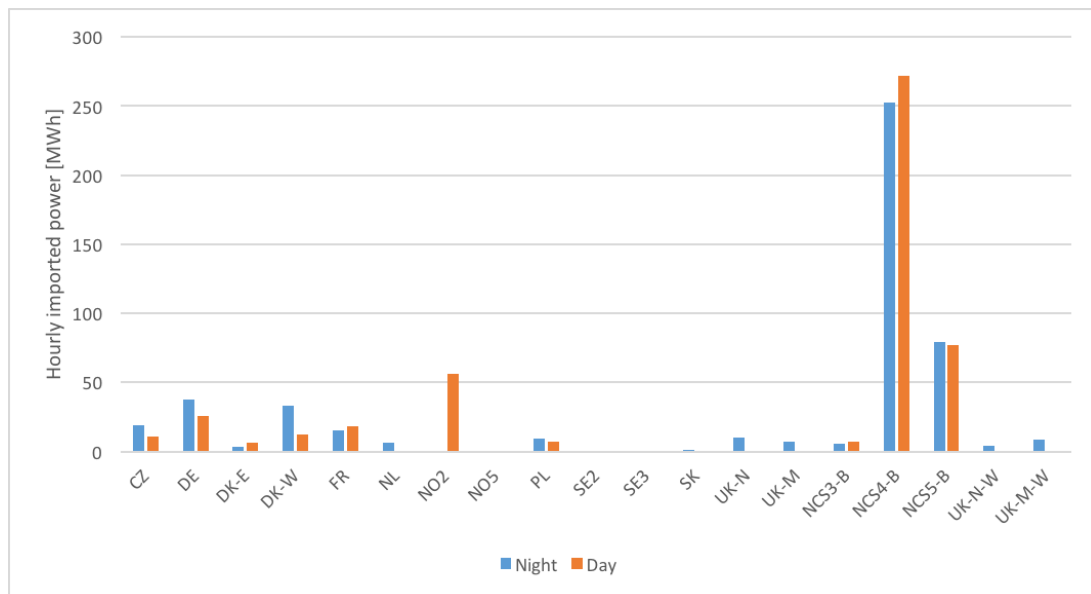


Figure 4.7: Imported energy to NCS4-A on January 1st, separated into contributing areas.

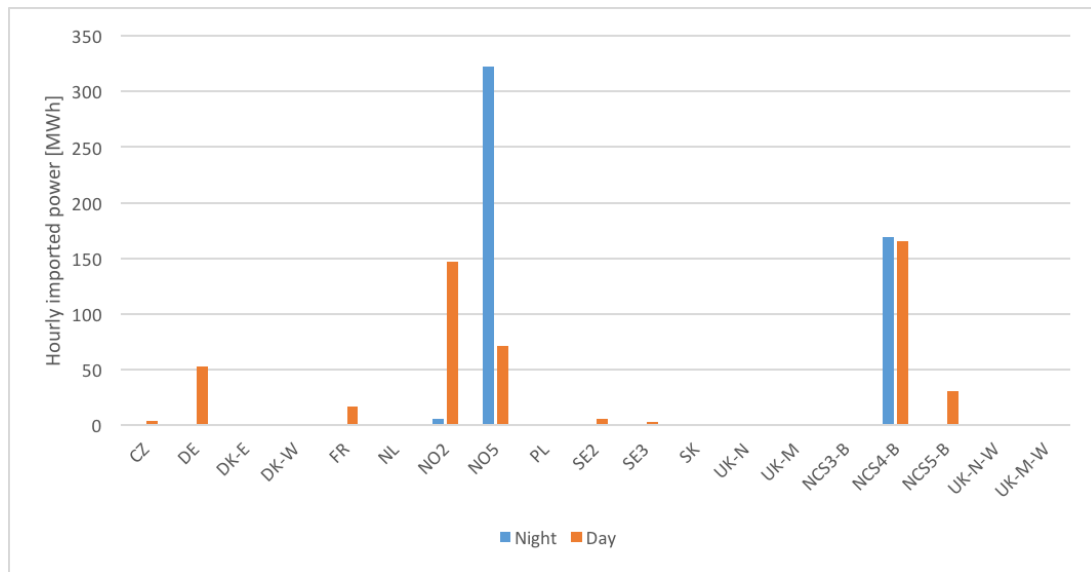


Figure 4.8: Imported energy to NCS4-A on July 1st, separated into contributing areas.

Apart from the fact that NCS4-A imports less from wind power producing areas (NCS4-B, NCS5-B, UK-N-W, UK-M-W) in the summer, due to less wind, and more from hydro power producing areas (NO2, NO5) in the summer, due to more water in the reservoirs, other additional information relating to Figure 4.7 and 4.8 may also be worth mentioning.

One of them is that during winter there is more import to NCS4-A from other countries during the night than during the day. Countries such as Germany (DE), The Czech Republic (CZ), Poland (PL), Netherlands (NL) and Denmark (DK) are using coal for heat through combined heat and power (CHP) plants during the winter. In such plants, electric power is a "by-product" in the winter, even though the intention is that the heat is the "by-product". Coal is cheap to use, but cannot be turned on and off efficiently. Therefore there will be a surplus of power in these countries when the demand goes down in the night, making the energy cheaper to import to Norway and by that profitable compared to our own hydro power plants. During the day this is not the case. The demand goes up, and the countries consume their own coal power in combination with gas. Gas power plants are easier to turn on and off. Due to less demand and more hydro power production in Norway during summer, this is only the case during winter.

It can also be seen in Figure 4.8 that during summer there is most import from NO2 to NCS4-A during the day, compared to the night. This is opposite for NO5. One reason for this could be that since NO5 is closer to NCS4-A, it is more profitable, due to transfer

losses, to produce the necessary power in NO5. This is in combination with an overall lower power demand in areas close to NO5 in the night, which makes more of the power produced in NO5 accessible for NCS4-A then. During the day, however, much of the power from NO5 is exported to other areas, which results in that NO2 must contribute more to NCS4-A.

Both NO2 and NO5 are dominated by hydro power, and even more specific hydro power from plants with reservoirs, which easily can be regulated. This makes it possible to choose when to produce energy. On the contrary NO1 is also dominated by hydro power, but there run-of-the-river hydro power plants are the most common[32]. Due to little or no storage capacity these power plants cannot be regulated easily, and therefore they produce the same amount of power day and night. This can be seen when comparing the export from NO1 in the night and in the day, on the 1st of July (Figure 4.9).

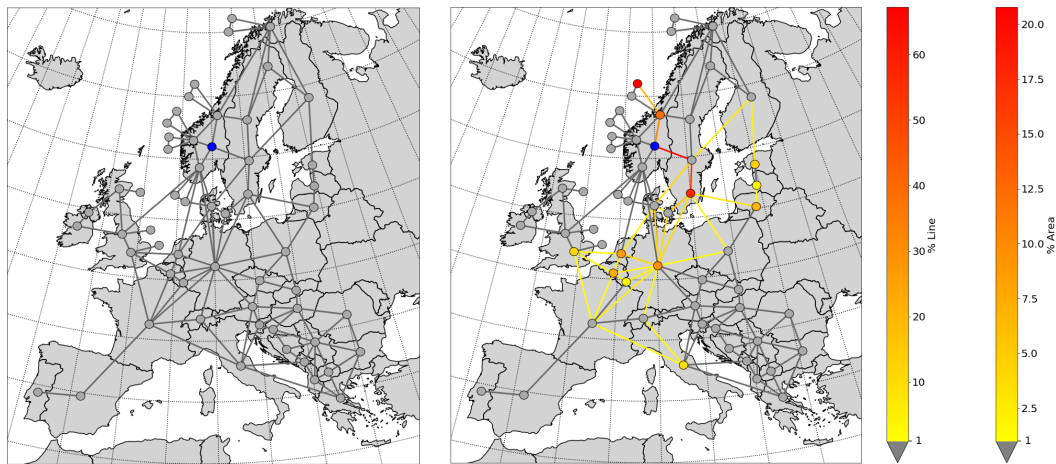


Figure 4.9: Export from NO1 in the day (left) and night (right) on July 1st.

As seen in Figure 4.9 there is no export from NO1 during the day in the summer. This is because the produced power is consumed by loads within NO1. The demand is lower in the night, and since the run-of-the-river plants produce the same amount the energy is exported. The areas that import this power are deficit areas, that need power due to for example no solar power production during the night. In the winter there is little or no production in these hydro power plants, which is why it is not presented an equivalent figure to Figure 4.9 for winter.

4.2.1 CO₂-coefficient in exporting areas

The share of imported energy to NCS4-A from the different areas vary, as shown, between winter and summer, and between night and day. This affects the amount of CO₂ that the total imported energy to NCS4-A is responsible for. The way that the CO₂-coefficient in the different areas change due to season and time of day, also affects the amount of CO₂. Two countries, or areas, that export energy to NCS4-A are Germany (DE) and France (FR). The CO₂-coefficient for the energy production in these areas are presented in Table 4.1.

Table 4.1: CO₂-coefficients [ton/GWh].

Time	Area	
	Germany (DE)	France (FR)
January 1 st , night	342.6	15.5
January 1 st , day	94.3	1.5
July 1 st , night	657.3	48.8
July 1 st , day	256.6	8.6

Table 4.1 shows that Germany has much higher CO₂-equivalents than France. This is because Germany produces most of its energy by burning coal, which stands for much emission, while France produces most of its energy with nuclear reactions, which stands for zero emission. The yearly production mix in the different countries can be seen in Appendix A.

Also, it can be seen that both countries have their highest equivalent during the night in July, and their lowest equivalent during the day in January. The reason that the highest equivalents are in July is that the power demand is lower in the summer than in the winter. This leads to lower power production in the summer than in the winter. Since coal (Lignite) is cheap it is prioritised over other power sources such as gas and nuclear, creating emission in both seasons. With less total production the coal stands for a greater share of the power in the summer. Also, the wind power production is higher in both areas in the winter than in the summer. Wind power does not hold any emission. A low CO₂-equivalent during the day can be explained by solar power. Both Germany and France have installed solar power, which only produce energy during the day. Solar power does not produce any emission, which contribute to a lower CO₂-equivalent.

4.3 Discussion

All of the results presented above were as expected, which strongly suggest that the PFT Model was successfully developed. One first and important indication that the model works as desired is that all lines with power flow are connected in the figures obtained with the Plot code in the PFT Model (Figure 3.2 to Figure 3.4, Figure 3.6 to Figure 3.10, and Figure 4.9). If the lines were not connected, KCL could not have been satisfied. The importance of KCL was pointed out in Section 2.2. Further, the results (both the Excel files from the PFT code and the figures from the Plot code) have been interpreted with sensible knowledge and known data of the power system, which strengthen the PFT Model's credibility.

The PFT Model gives results both for each hour and as an average of the chosen hours, which gave the opportunity to analyse data both for yearly average, and for seasonal and daily differences. The seasonal and daily variations in the European energy system have been explained with weather and climate, but it should be noted that two specific hours in two specific days have been used in the comparisons. Other days could have very different situations concerning e.g. wind and rain, which could affect the power production in different areas, and by that the CO₂-equivalents and energy flow in the power system.

Something else that could have affected the results are the limitations presented in Section 3.2. The assumptions of nodes being perfect mixers and loads being handled locally cannot be validated with today's information and technology, and it may never be possible. As also cited in Section 2.2.1, it is simply "impossible to 'dye' the incoming flows and check the colour of the outflows"[4]. The limitation of equivalent networks, however, can be proven.

It is generally known that power systems rarely are without loss. Still, Bialek's algorithm assumes lossless systems. The equivalent networks which are made to meet this demand deviates little from the actual power system, which leads to results with some degree of insecurity. As seen in Section 3.1.4 the validation with the base case scenario did reveal differences in total flow from the EMPS 3 Model and the PFT Model. This was as expected. Still, the differences was so small (maximum 3.00%) that it is reason to conclude that this limitation does not affect the results considerable. The results from the upstream-looking algorithm and the downstream-looking algorithm should be considered together. The first one allocates loss to loads and has right values for generation, while the second one allocates loss to generators and has right values for demand.

4.4 Impact of results

The direct meaning of the results from the PFT Model have been explained and discussed, but how relevant and advantageous they are is just as important to discuss. Whether the scenarios are realistic is uncertain. Also, whether it is right to use the offshore wind power to replace gas and to allocate expenses according to Bialek's algorithm, is uncertain.

4.4.1 Building of scenarios

Before the simulations in EMPS was done, the scenarios had to be built. For the partial- and full electrification scenarios a big scale offshore wind development was used, where all areas investigated by NVE were included. The time frame for the wind developments was set according to their potential. For the electrification it was decided that all platforms with three or more expected years until shutdown were electrified, either completely in the full electrification scenario or partial in the partial electrification scenario. The time frame for the electrification was set relatively short and it was pre-defined that all platforms would be electrified within 2025.

Both the offshore wind power development and the electrification of the platforms are quite optimistic in magnitude, and it might not be realistic. It is expensive to carry out such comprehensive projects, but this was not taken into account when building the scenarios. Expenses are, however, an important factor in industrial development, such as offshore electrification. Due to this it is possible that the resulting impact of the electrification is, as presented in this thesis, not very relevant. At least not in 2025. It was, however, decided to include everything in order to give extreme situations, which showed the trends clearly.

Something else which might not be realistic is the choice of power system scenario. Choosing Current Policies (CP) is, unlike the development of electrification scenarios, pessimistic. Hopefully, and most likely, new policies will be implemented with the goal of reversing the climate crisis. Choosing New Policies (NP) instead would most likely give a more relevant result, but as mentioned in Section 2.1.3 would it not affect the impact in 2025 significantly.

4.4.2 Alternative usage of offshore wind power

The results from the PFT Model have shown the import and export from the NCS in case of electrification. None of the constructed scenarios show a power system with only offshore wind power on the NCS, they have either nothing on the NCS or wind power

in combination with a degree of electrification of platforms. It is, however, of interest to see where the offshore wind power would have been consumed if it were not for the platforms. Since coal emits more GHG than gas it would be preferable if the wind power was used to decrease coal power production.

A project carried out by SINTEF Energy shows, among other things, how production of 3 TWh offshore wind energy on the NCS affects the energy system, when there are no other alterations. The result from this study, which is dependent on production prices and transfer capacities, can be seen in Table 4.2[33].

Table 4.2: Difference in production, consumption, import and export [GWh] between SINTEFs wind scenario and base scenario[33].

	Country									Sum
	Norway	Sweden	Denmark	Finland	UK	Germany	Netherlands	Belgium	Others	
Hydro	-69	12		-2	0	0			0	-60
Wind	3000	0	0	0	0	0	0	0	0	3000
Bio		-599	-107	-173	-1	-110	-8	-15	0	-1013
Coal			-133	-231	-8	-427	-150		-424	-1374
Gas	-30	-17	-20	-6	-1	-5	-68	-11	-428	-584
Oil		-27	-1	0		0	0		0	-29
Nuclear		-77		-14	0	-4	0	0	1	-95
Production	2901	-708	-262	-427	-10	-546	-226	-26	-851	-156
Consumption	62	33	15	9	2	9	10	0	-299	-159
Export	1390	-492	88	-61	-2	141	175	-5	-110	1125
Import	-1448	251	364	375	9	698	413	22	442	1125
Net. export	2839	-744	-276	-436	-10	-557	-237	-26	-552	0

In Table 4.2 it can be seen that an increase in wind power production in Norway leads to a decrease in mainly power production from bio fuel and coal. Since the new production of wind energy firstly replaces the most expensive power plant, is it not necessarily the one with greatest emission that gets reduction. Replacement of power from coal is as desired, but replacement of bio power is unnecessary. Burning of bio fuel does not emit GHG, so replacing bio energy with wind energy does not give any benefit concerning emission. The fact that power from bio fuel is replaced indicates that the bio fuel price is higher than or equal to the price of coal combined with its associated CO₂-price. Also, most of the bio energy which is replaced is in Sweden, which is natural since it is close. By reducing the power production in Sweden, more power is exported from Norway to

Sweden. Table 4.2 also shows that sending all offshore wind power out in the power system leads to a small decrease in hydro power in Norway. This is unfortunate. If it were not for the maxed capacities in the lines leading to UK and Finland, more energy would, most likely, be transferred there as well, due to higher area prices[33]. With a higher CO₂-price the price of coal would be even higher, leading to more coal being replaced. This is because, like mentioned in Section 1.1, the power system works as a competitive market.

This thesis does not take into account where the gas, which is saved when electrifying the platforms, is burned instead. Gas is better than coal concerning emission, and if the saved gas is used to replace coal in for example Germany, the total emission would be lower than what is simulated here. This makes it difficult to say whether it is best to send the wind power, rather than more gas, to other European countries. More gas in Germany could potentially lower the country's CO₂-coefficients and by that total European emission.

4.4.3 Disadvantages for geographical positions

As mentioned in Section 2.2.3 the postage stamp method, or pro rata method, is a common way of allocating losses. This method does not differentiate consumers by how much they use transmission facilities. Cost of losses is rather allocated based on the amount of transacted energy. This results in that the ones with short electrical distance, and by that uses the transmission system lightly, will subsidise the ones with long electrical distance. The method is simple and does not require any assumptions, since in theory it ignores the power network. It is, however, argued that it is unfair and little efficient[29].

The tracing method presented and used in this thesis, developed by Bialek, makes it possible to charge users for the actual loss they cause in the power grid. The further energy has to travel, the more loss it causes. This improves efficiency, but at the same time raises questions whether users should be penalised for their geographical position[4]. By allocating losses also to the producers, which is possible with Bialek's method, does the location of these generators becomes essential as well. Since especially producers of renewable energy, such as hydro power and wind power, cannot decide about their location, they get the disadvantage of extra costs. The location of the natural reasons decides where they can be built.

Both methods (postage stamp method and Bialek's tracing method) raise dilemmas. While it is unfair that actors who do not use the transmission system much must sub-

sidise others, it can also be unfair that actors located further from source points must be penalised for it. In Norway the cost of losses is mostly allocated to consumers by TSOs, by the principle of postage stamp method. Consumers are invoiced with one fixed amount and one variable amount. The fixed one includes specific expenses such as maintenance and development, and the variable one includes marginal costs such as transmission losses. The marginal costs are the same for everyone within the specific geographical area[34]. Whether this is the best way of financing the cost of the power grid, and whether both producers and consumers should be invoiced for the power loss, is up for discussion. This also applies to the dilemma of emission: should consumers be invoiced according to how "dirty" the electricity in their sockets is?

Chapter 5

Concluding Remarks

In this Master's thesis the method of Power Flow Tracing has been explained in theory and implemented in Python as part of a model called the PFT Model, and the model worked as expected. After the PFT Model was verified and validated, it was demonstrated by investigating how the European energy system would react to electrification. A tool, such as this model, which makes it possible to tell where power flows to/from, and that allocates losses, is very useful. As mentioned in the motivation SSB and NVE use less detailed methods in their attempts of documenting emission, which leads to unnecessary insecurity. The PFT model could help with that.

There is potential for using this model further for studies both within the topic of electrification, and for other topics in other parts of the energy system. It can be used as it is, or be further developed for improved workability. This will be discussed. First, however, a summary of the results from the simulations and the analysis of it will be given.

5.1 Summary of results

The results in Chapter 4 show information about how the European energy system would react to an electrification of oil- and gas platforms, both in terms of yearly average, seasonal variations and daily variation. The area in focus is the NCS, more specifically a cluster of oil- and gas platforms called NCS4-A, which is located south west of the Norwegian coast. This area imports most of its energy, when electrified, from other areas on the NCS and areas in Norway. Still, most of the emission associated with the consumption at NCS4-A origins from Germany and The Czech Republic, which are countries that have much coal power.

Looking at NCS4-A isolated shows that even though some of the imported power is produced with coal, the total emission associated with the platforms is lower when electrifying them. This became clear when comparing the partial- and full electrification scenarios. It is, however, important to consider the whole of Europe. For the total European emission the partial electrification scenario is actually better than the full electrification scenario, which reveals that it exists an optimal degree of electrification, and this is not completely electrification.

When comparing winter and summer the seasonal climate variation became visible. There is more wind in the winter and more water in reservoirs in the summer. Also, an indirect consequence of cold weather that became clear when comparing night and day in the winter, was that countries in central Europe fire coal in CHP plants for heat. Since there is more power available in the night than during the day in these countries, due to lower demand, NCS4-A imports more power from them in the night. In the summer the daily variation is mostly linked to which Norwegian hydro plant area that feeds NCS4-A with power. During the night the closest one, NO5, can contribute with more than during the daytime due to more available power.

The climate/weather variations do also affect the CO₂-coefficients, which are shown when comparing both winter and summer, and night and day. In Germany and France, which are the areas analysed, the equivalents are highest in the night in the summer, and lowest in the day in the winter.

5.2 Future work

Because of the time limitations for the master program, the scope of this thesis had to be limited. This results in that there are other aspects of the theme and model which could be included in potential further work. Four examples of this are to use the PFT Model for reactive power flow tracing, to analyse different scenarios of policies and electrification, to improve the PFT code for dealing with parallel lines, and finally to further develop the PFT Model such that it can handle input files with different shapes and scopes.

5.2.1 Reactive Power Flow Tracing

Since output from the EMPS model, which was used as input to the PFT Model, only has active power flow, reactive power flow was not included as a part of this thesis. The presented PFT algorithm is also applicable on reactive power flow, as the only requirement is that KCL is obtained. As mentioned in Section 2.2.3 the line loss of reactive

power is higher than it is for active power. This indicates that the simplifications for active power flow, which states that $\frac{|P_{j-i}^{\text{gross}}|}{P_j^{\text{gross}}} \approx \frac{|P_{j-i}|}{P_j}$ and $\frac{|P_{j-i}^{\text{net}}|}{P_j^{\text{net}}} \approx \frac{|P_{j-i}|}{P_j}$ and is used in Section 2.2.3, cannot be directly transferred to reactive power flow. It would actually be invalid. In addition, using average power flow instead would also cause difficulties.[4]

In order to deal with reactive power flow in the PFT algorithm additional nodes would have to be added to the system, acting as fictitious reactive power sources or sinks, placed in the middle of transfer lines. These additional nodes would be responsible for line generation or line consumption. The PFT code can be expanded to handle this in future work, which would be useful for system operations and reactive power pricing[4].

5.2.2 Different scenarios

The power system scenario which was chosen is Current Policies (CP). This was done with the justification that the other power system scenarios might give results not directly linked to the adjustments done when building the scenarios. It would be interesting to see how the system would behave with the New Policies (NP) scenario and the 450 ppm (450) scenario. Still, as pointed out in Section 2.1.3, this would probably not give considerable changes in the simulations for 2025.

Also, in this thesis the full electrification scenario in 2025 was chosen as main focus, and in some situations it was compared to the partial electrification in 2025. It could be interesting to compare the flow to scenarios in 2045. Also, it could be interesting to simulate scenarios with electrification of other parts of the power system, such as battery factories or transportation. These are only examples, and there exist almost an unlimited amount of different scenarios which could be analysed, both with the EMPS model and the PFT Model.

5.2.3 Parallel lines

The EMPS 3 model, shown in Figure 2.1, does not have any parallel lines. Some cross country power connections, such as the Skagerrak HVDC transmission system between Norway and Denmark, consist of parallel transfer lines. The Skagerrak system comprises four lines which make out 1,700 MW transmission capacity. Skagerrak 1-3 are 127 km, while Skagerrak 4 is 140 km (submarine cable routes)[35]. Different lines leads to different properties concerning transferred power and loss. For further work it could be useful to either merge lines in the code itself, conditioned that the input data take into account parallel lines, or to analyse the lines closer by for example comparing tracing results before and after a power system outage in one or more of these lines.

5.2.4 Universal code

The PFT Model, more specific the PFT code, is very dependent on the input files having a specific form, as it is now. Other simulation programs than EMPS, for example PowerGAMA[36], can produce files which holds the same kind of information (power flow on branches, production etc.), but with dissimilar setup. It could be useful to improve the PFT Model in such a way that it is universal, and hence is able to import files with different shapes. The code would need to recognise headers and directions (vertical/horizontal), in order for it to work as desired.

For the visualisation in the Plot code it is necessary to have coordinates for both the drawing of map and the marking of areas. A universal code could hold a library of more coordinates than the PFT Model and make it possible to choose the scope of simulation. It requires more work, but should not be too hard with the PFT Model as foundation.

References

1. I. Wangensteen. *Power System Economics - the Nordic Electric Market* (Tapir Academic Press, Trondheim, 2nd edition, 2012).
2. Ministry of Petroleum and Energy. "Act no. 50 of 29 June 1990: Act relating to the generation, conversion, transmission, trading, distribution and use of energy etc (The Energy Act)". https://www.regjeringen.no/globalassets/upload/oed/vedlegg/lover-og-reglement/act_no_50_of_29_june_1990.pdf (1990).
3. ENTSO-E. *Electricity Market Transparency [Online]* <https://www.entsoe.eu/data/transparency-platform/>. (Accessed: March 2. 2021).
4. J. Bialek. "Tracing the flow of electricity". *IEEE Proceedings General Transmission Distribution, Vol. 143, No. 4, p. 313-320* (feb. 1996).
5. Statistics Norway(SSB). *Emission to air [Online]* <https://www.ssb.no/en/natur-og-miljo/statistikker/klimagassn>. (Accessed: April 29. 2021).
6. The Norwegian Water Resources and Energy Directorate(NVE). *Hvor kommer strømmen fra? [Online]* <https://www.nve.no/energiforsyning/kraftproduksjon/hvor-kommer-strommen-fra>. (Accessed: May 3. 2021).
7. I. E. Wibe. "Impact of offshore electrification in Norway to greenhouse gas emission within the European energy system," *Specialisation project, Department of Electric Power Engineering, NTNU, Trondheim* (2020).
8. Regjeringen. *Klimaendringer og norsk klimapolitikk [Online]* <https://www.regjeringen.no/no/tema/klima-og-miljo/innsiktsartikler-klima-miljo/klimaendringer-og-norsk-klimapolitikk/>. (Accessed: April 29. 2021).
9. Equinor. *Equinor aims to cut emissions in Norway towards near zero in 2050 [Online]* <https://www.equinor.com/en/news/2020-01-06-climate-ambitions-norway.html>. (Accessed: April 29. 2021).

10. A. Bjartnes. *Elektrifisering av oljesektoren: Her er et forsøk på å gi et faktagrunnlag for debatten* <https://energiogklima.no/kommentar/klimavalg21/elektrifisering-av-oljesektoren-her-er-et-forsok-pa-a-gi-et-faktagrunnlag-for-debatten/>. (Accessed: April 29. 2021).
11. A. Reyes-Lúa, et al.. "Electric power and heat systems on oil and gas platforms on the Norwegian Continental Shelf". *SINTEF Energy Research (LowEmission Research Centre), Trondheim, Norway, Tech. Memo. No. 1* (des. 2019).
12. Oljedirektoratet. "Kraft fra land til norsk sokkel". *NPD, Stavanger, Norway* (2020).
13. SINTEF Energy Research. "The EMPS model - part 1," user manual.
14. L. Riboldi, et al.. "An Integrated Assessment of the Environmental and Economic Impact of Offshore Oil Platform Electrification". *Energies. vol 12 (11), No. 2114* (jun. 2019).
15. M. Ulvensøen. "Changes in the European energy system, resulting from increase in Norwegian transmission capacity and hydropower development," *Master's thesis, Department of Electric Power Engineering, NTNU, Trondheim* (2019).
16. Oljedirektoratet. "Oversiktskjema for NO_x-avgiftspliktig utstyr," Excel file (2012).
17. K. S. Berg, et al.. "Havvind - Strategisk konsekvensutredning". *The Norwegian Water Resources and Energy Directorate(NVE), Oslo, Norway, 47-12* (dec. 2012).
18. F. Birol et. al.. "World Energy Outlook 2016". *International Energy Agency(IEA), Paris, France* (nov. 2016).
19. United States Environmental Protection Agency(EPA). *Overview of Greenhouse Gases [Online]* <https://www.epa.gov/ghgemissions/overview-greenhouse-gases>. (Accessed: June 4. 2021).
20. Energi Norge. *Spørsmål og svar om opprinnelsesgarantier [Online]* <https://www.energinorge.no/tall-og-fakta/sporsmal-og-svar/>. (Accessed: March 16. 2021).
21. G. A. Orfanos, et al.. "Evaluation of Transmission Pricing Methodologies for Pool Based Electricity Markets". *IEEE Trondheim PowerTech, Trondheim, Norway* (jun. 2011).
22. K. Berg. "Power Flow Tracing: Methods and Algorithms," *Master's thesis, Department of Electric Power Engineering, NTNU, Trondheim* (2017).
23. B. Khan, G. Agnihotr. "A Comprehensive Review of Embedded Transmission Pricing Methods Based on Power Flow Tracing Techniques". *Hindawi Publishing Corporation, Chinese Journal of Engineering, vol. 2013, No. 501587* (aug. 2013).

24. Z. Jing, F. Wen. "Discussion on the Proving of Proportional Sharing Principle in Electricity Tracing Method". *2005 IEEE/PES Transmission and Distribution Conference and Exhibition: Asia and Pacific, Dalian, China* (aug. 2005).
25. D. Kirschen, et. al.. "Contributions of Individual Generators to Loads and Flows". *IEEE Transactions on Power Systems, Vol. 12, No. 1, p. 52-60* (feb. 1997).
26. S. Nojeng, et al.. "Novel Approach for Determination of Generator Contribute in Transmission Usage Based On the Average Tracing Method". *International Conference on Electrical, Mechanical and Industrial Engineering(ICEMIE 2016)*, p. 143-145 (apr. 2016).
27. S. Abdelkader. "Determining generators' contribution to loads and line flows losses considering loop flows". *International Journal of Electrical Power and Energy Systems, Vol. 30, No. 6 p.368-375* (jan. 2008).
28. J. Bialek. "Identification of source-sink connections in transmission networks". *Fourth International Conference on Power System Control and Management (Conf. Publ. No. 421)*, p. 200-204, (apr. 1996).
29. C. Singh, et al.. "Transmission Loss Allocation: Comparison of Different Methods". *International Journal of Advanced Research in Electrical, Electronics and Instrumentation Engineering, Vol. 3, p. 9386-9393* (may 2014).
30. H. Farahmand, et al.. "Task 16.3. Nordic hydro power generation flexibility and transmission capacity expansion to support North European wind power: 2020 and 2030 case studies". *SINTEF Energy Research (TWENTIES Project)* (mar. 2013).
31. Store norske leksikon. *Vind [Online]* <https://snl.no/vind>. (Accessed: April 15. 2021).
32. P. Sanderud, et al.. "Skattlegging av vannkraftverk". *Norges offentlige utredninger(NOU), No. 16, Oslo, Norway* (sep. 2019).
33. S. Völler, et al.. "Energi- og miljøpåvirkning av elbil, systemanalyse med EMPS (Samkjøringsmodellen)". *SINTEF Energy Research, Vol. 1, No. TR A7385, Trondheim, Norway* (feb. 2014).
34. The Norwegian Water Resources and Energy Directorate(NVE). *Nettleie for forbruk [Online]* <https://www.nve.no/reguleringsmyndigheten/nettjenester/nettleie/nettleie-for-forbruk/>. (Accessed: May 10. 2021).
35. Hitachi ABB Power Grids. *Skagerrak [Online]* <https://www.hitachiabb-powergrids.com/references/hvdc/skagerrak>. (Accessed: May 13. 2021).

36. H. Svendsen. *PowerGAMA er en åpen kildekode-python-pakke for kraftanlegg og markedsanalyser [Online]* <https://www.sintef.no/programvare/powergama-er-en-åpen-kildekode-python-pakke-for-kraftanlegg-og-markedsanalyser/>. (Accessed: June 1. 2021).

Appendix A

Background data

Information about offshore installations in Norway and UK

Table A.1: Energy consumption in areas with oil fields.

Area	Consumption in 2025 [GWh]	Consumption in 2045 [GWh]
NCS1-A	2940	360
NCS2-A	7277	0
NCS3-A	8144	1118
NCS4-A	4282	1982
NCS5-A	2498	1271

Table A.2: Installed power capacity in areas with gas turbines.

Area	El. capacity [MW]	Mec. capacity [MW]	Total capacity [MW]
NCS1-A	525	0	525
NCS2-A	1455	384	1839
NCS3-A	1830	523	2353
NCS4-A	747	211	958
NCS5-A	465	258	723

Table A.3: Installed power capacity in areas with offshore wind turbines.

Area	Installed capacity in 2025 [MW]	Installed capacity in 2045 [MW]
NCS1-B	300	1500
NCS2-B	350	4250
NCS3-B	200	2000
NCS4-B	1590	1590
NCS5-B	2000	3500
UK-N-W	1986	4861
UK-M-W	4084	12270
UK-S-W	1787	1787

Production mix in different scenarios in 2025

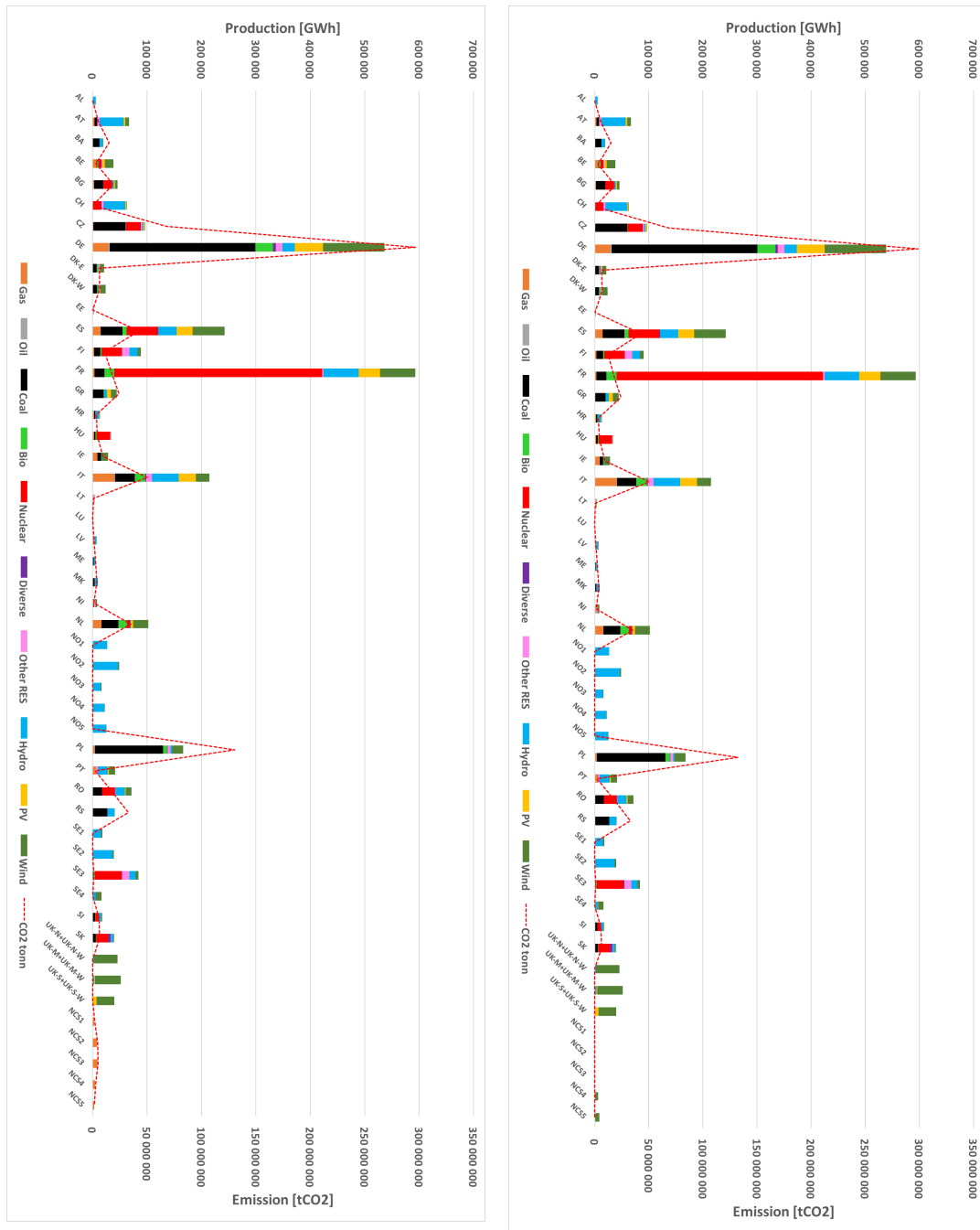


Figure A.1: Production mix: Base case in 2025 (left) and full electrification in 2025 (right).

Appendix A. Background data

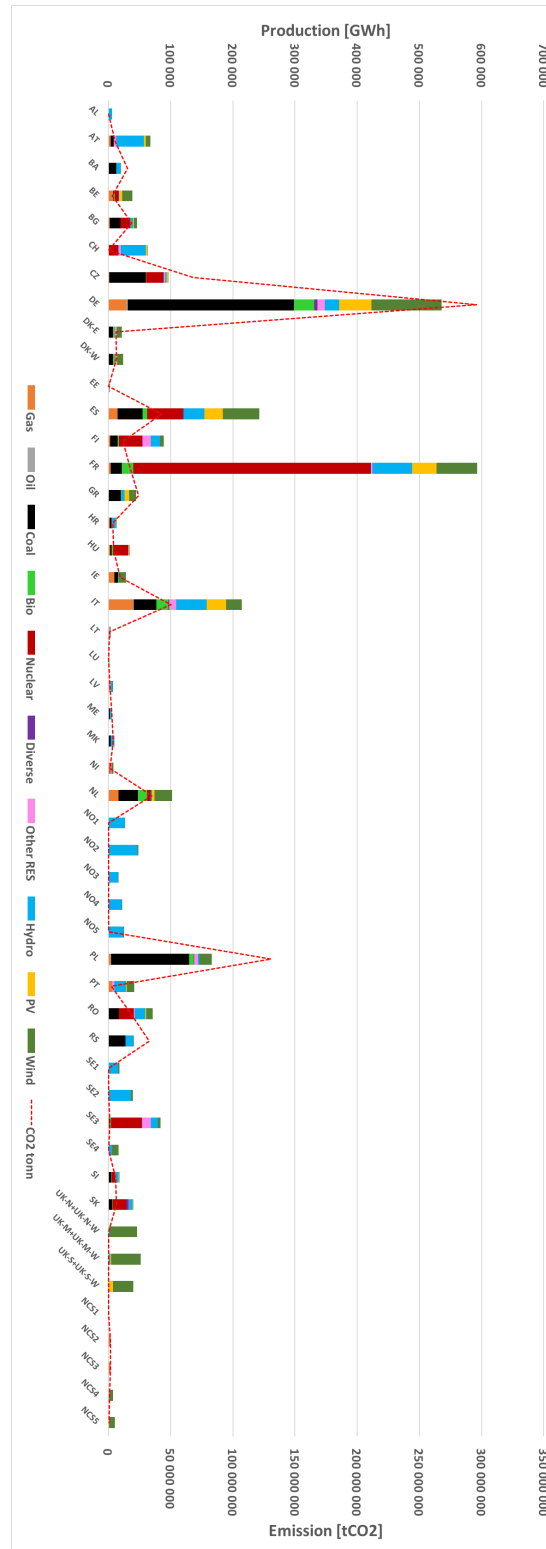


Figure A.2: Production mix: Partial electrification in 2025.

Difference in production mix between scenarios in 2025

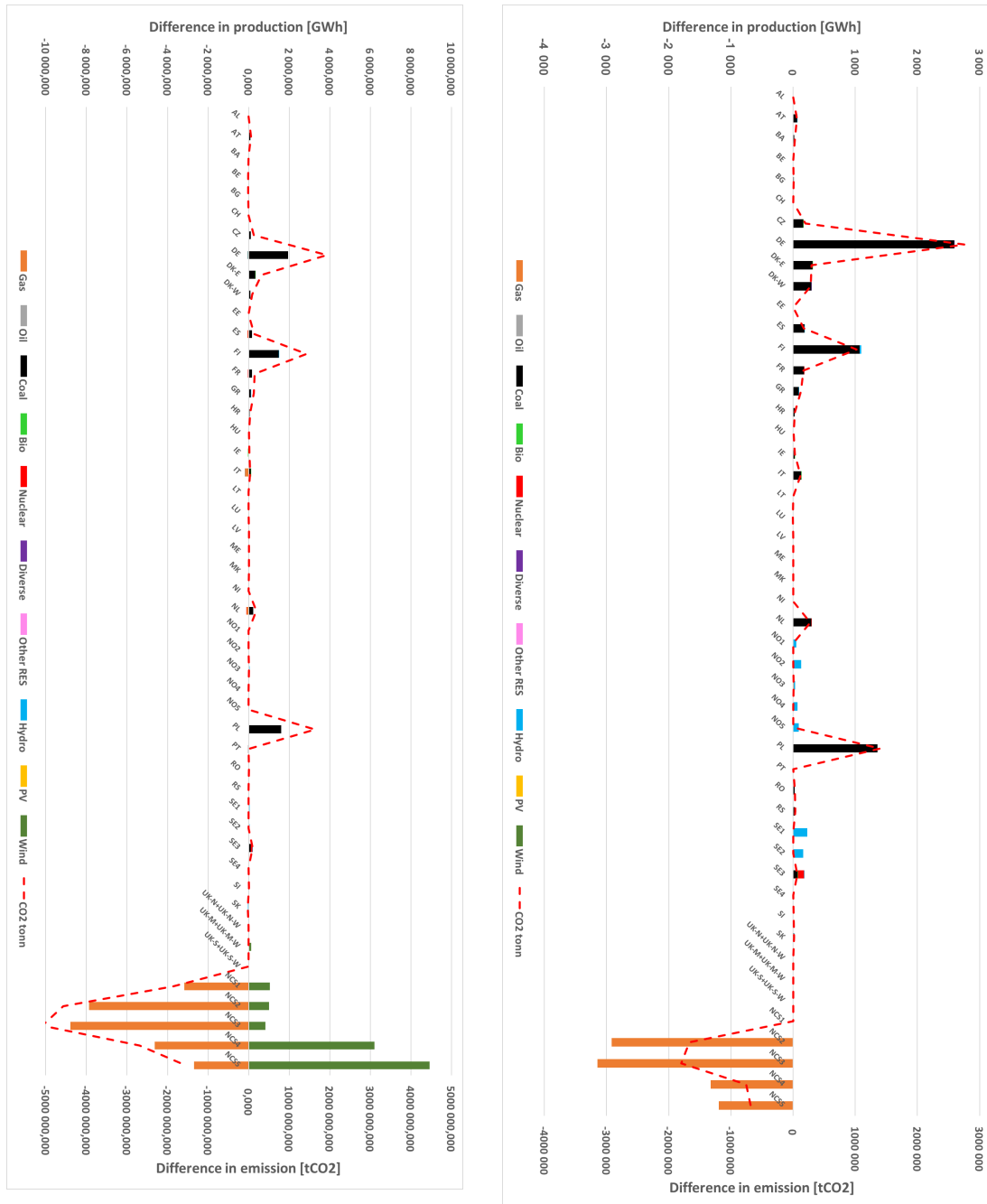


Figure A.3: Difference in production mix: Base case vs full electrification in 2025 (left) and Partly vs full electrification in 2025 (right).

Power flow to/from Norway in scenarios in 2025

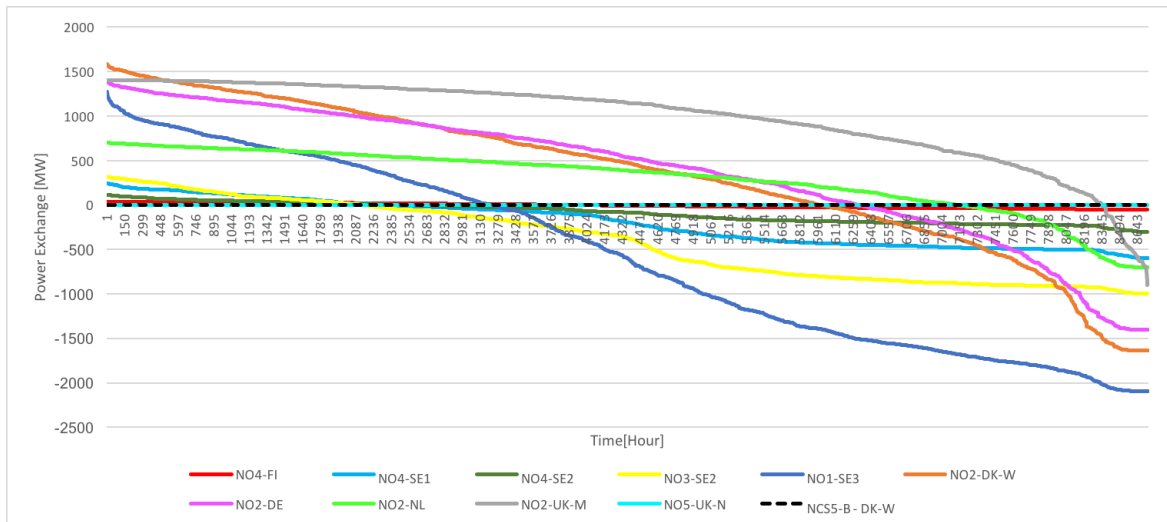


Figure A.4: Power exchange with neighbour areas in base case scenario in 2025.

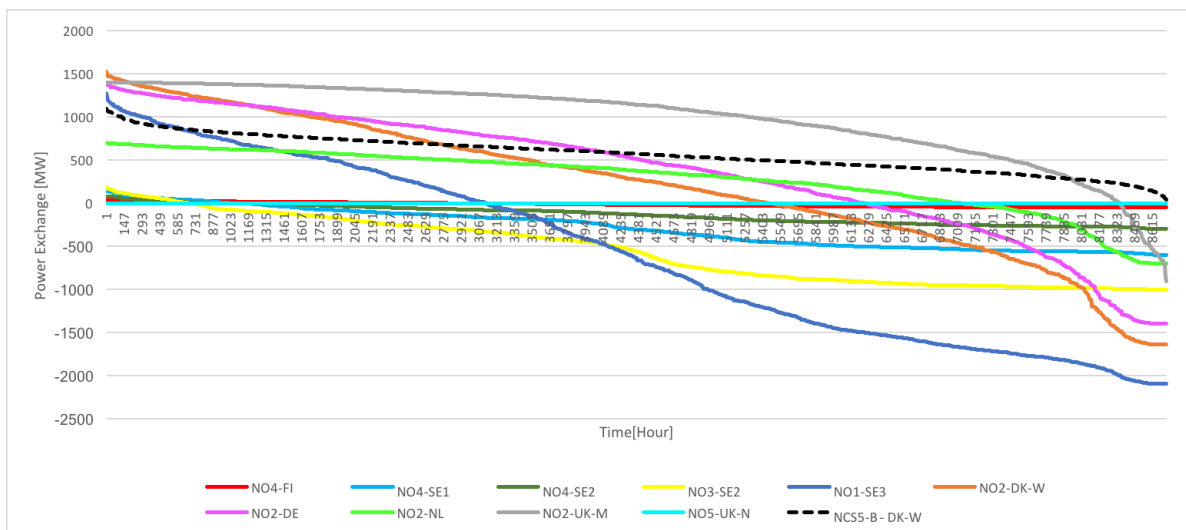


Figure A.5: Power exchange with neighbour areas in partial electrification scenario in 2025.

Appendix A. Background data

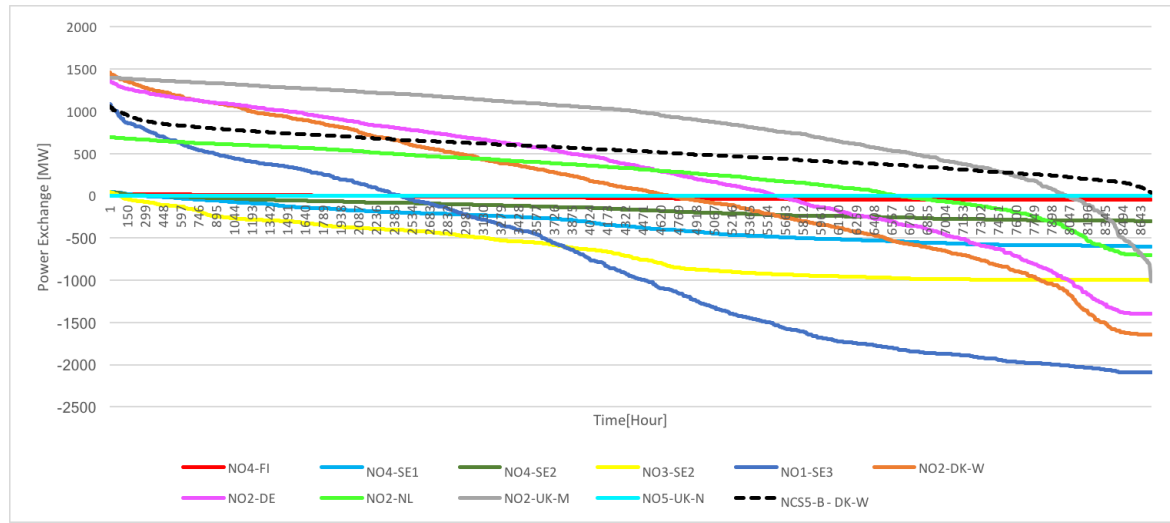


Figure A.6: Power exchange with neighbour areas in full electrification in 2025.

Appendix B

Six Bus Test System

Name on nodes in the Six Bus Test System

- Node 1 = "En"
- Node 2 = "To"
- Node 3 = "Tre"
- Node 4 = "Fire"
- Node 5 = "Fem"
- Node 6 = "Seks"

Results from using the PFT Model (upstream-looking algorithm) on the Six Bus Test System

Table B.1: Contribution of generators to loads.

gen/load	En	To	Tre	Fire	Fem	Seks
En	0	0	51.186	0	4.702	4.723
To	0	0	36.071	41.662	16.103	16.175
Tre	0	0	0	0	0	0
Fire	0	0	0	0	0	0
Fem	0	0	0	0	0	0
Seks	0	0	0	0	0	0

Table B.2: Contribution of generators to lines.

gen/line	En-To	En-Tre	To-Fire	Tre-Fire	Tre-Fem	Fire-Fem	Fem-Seks
En	0	60.61	0	0	9.424	0	4.723
To	-33.33	33.33	76.68	-9.382	6.641	25.636	16.175
Tre	0	0	0	0	0	0	0
Fire	0	0	0	0	0	0	0
Fem	0	0	0	0	0	0	0
Seks	0	0	0	0	0	0	0

Table B.3: Allocation of loss to loads.

	Loss
En	0
To	0
Tre	2.257
Fire	1.652
Fem	0.804
Seks	0.898
Total loss	5.61

Appendix C

Power flow to/from offshore installations in Norway

Yearly average power flowing towards offshore platforms (downstream-looking algorithm), full electrification scenario

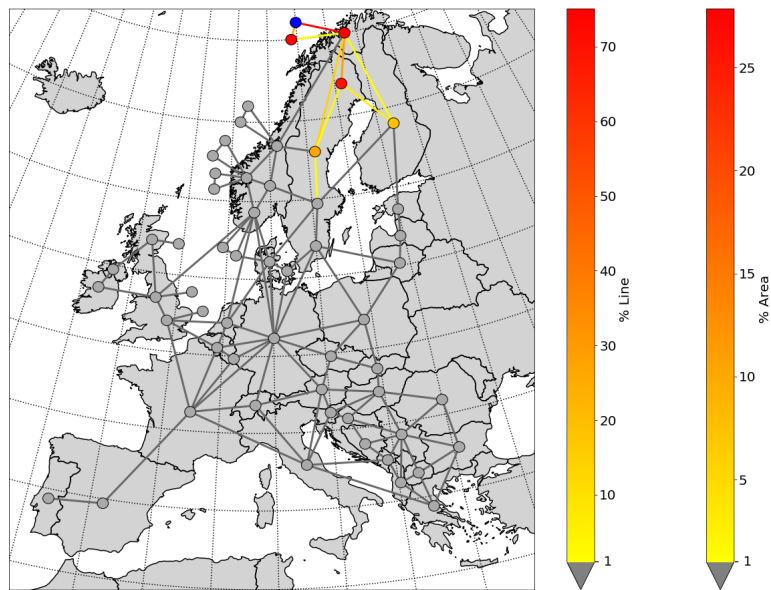


Figure C.1: Yearly average flow towards NCS1-A.

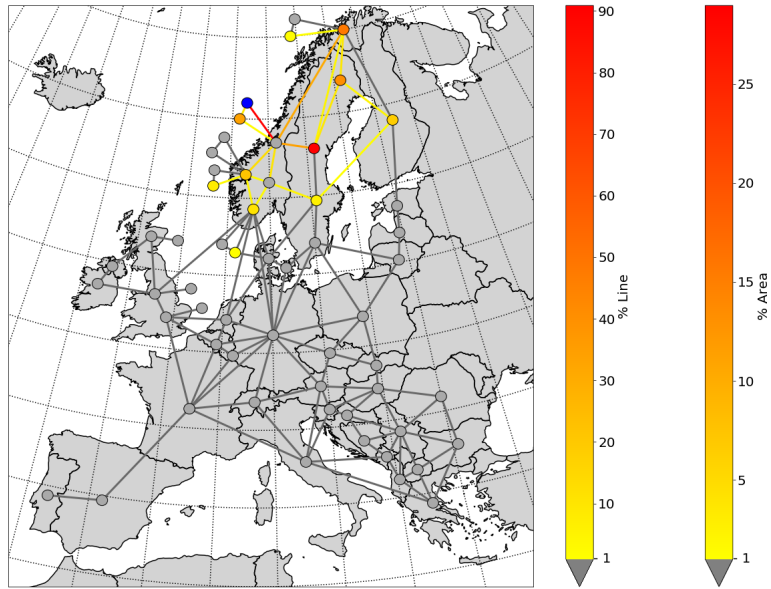


Figure C.2: Yearly average flow towards NCS2-A.

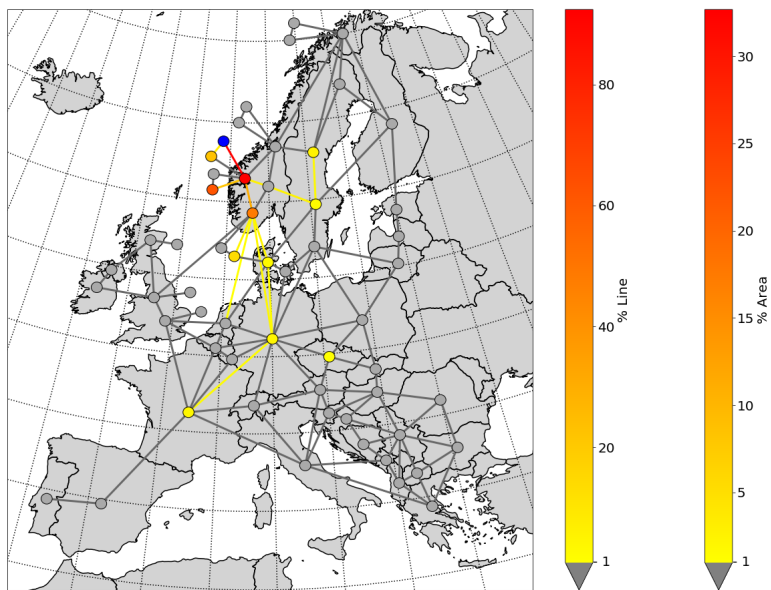


Figure C.3: Yearly average flow towards NCS3-A.

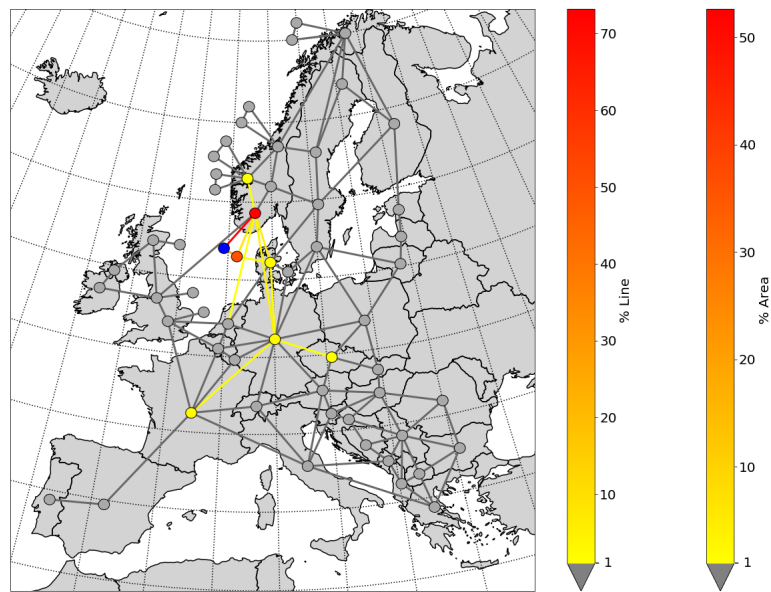


Figure C.4: Yearly average flow towards NCS5-A.

Yearly average power flowing from offshore wind turbines (upstream-looking algorithm), full electrification scenario

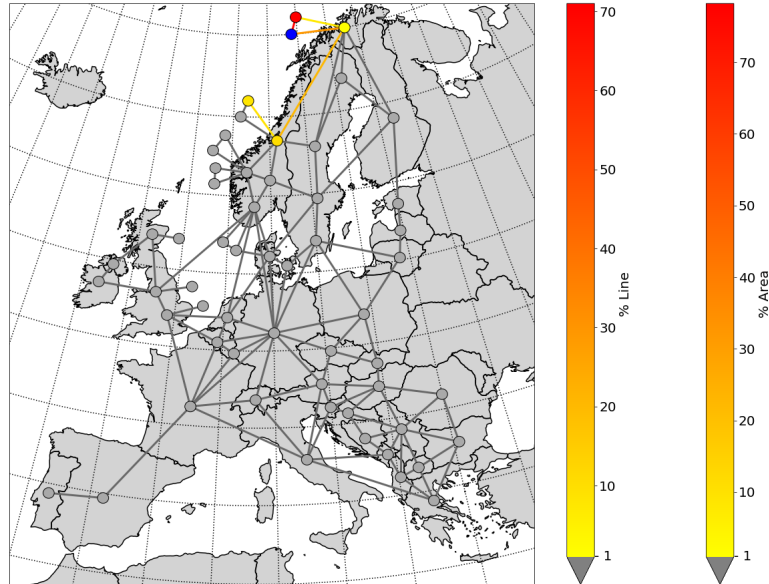


Figure C.5: Yearly average flow from NCS1-B.

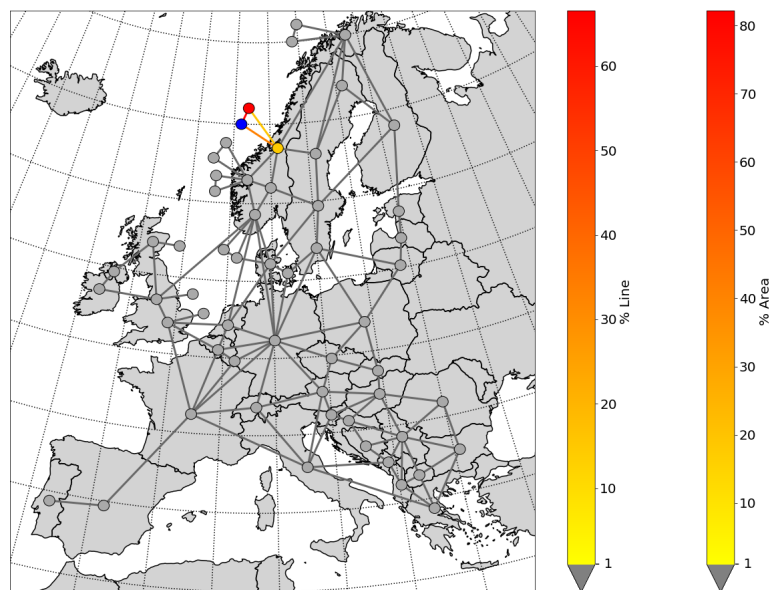


Figure C.6: Yearly average flow from NCS2-B.

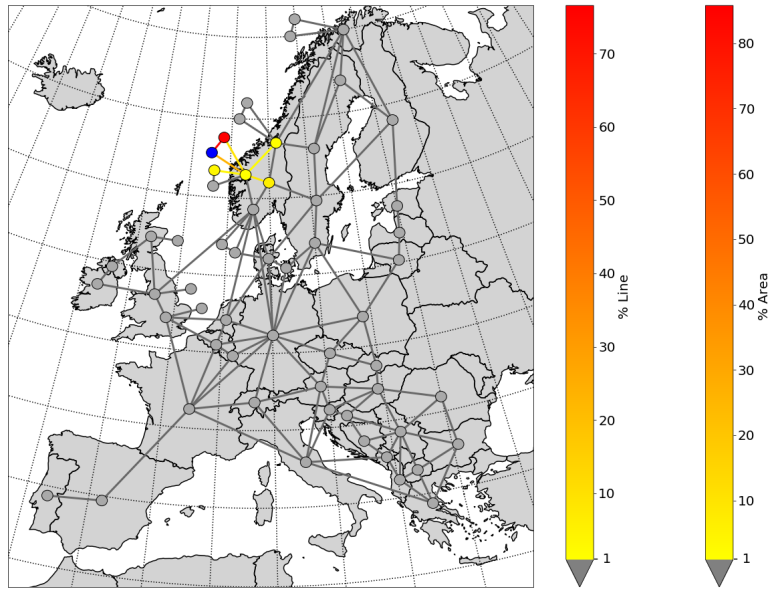


Figure C.7: Yearly average flow from NCS3-B.

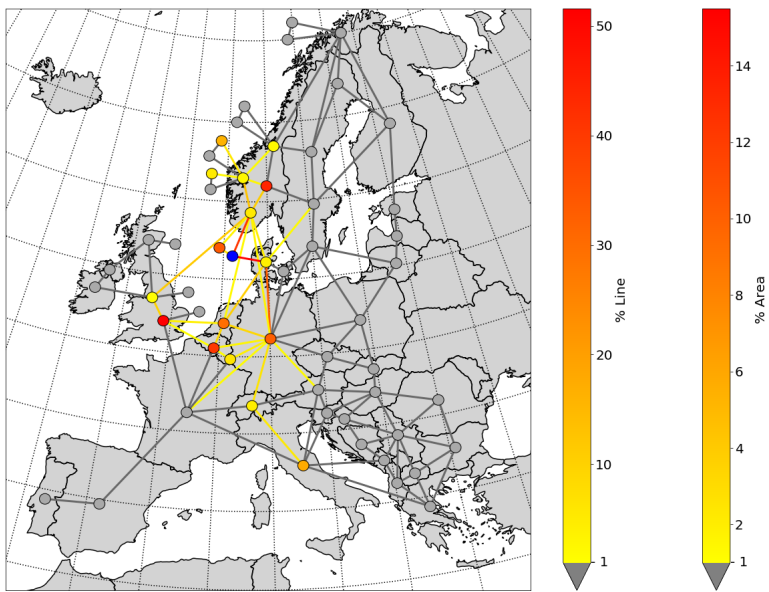


Figure C.8: Yearly average flow from NCS5-B.

Appendix D

Imported power to NCS4-A and CO₂-coefficients

Table D.1: Contributing areas to yearly average energy imported, and its associated emission, to NCS4-A in full- and partial electrification.

Generator/Scenario	Full electrification		Partial electrification		Difference	
	MWh/h	Ton CO2	MWh/h	Ton CO2	MWh/h	Ton CO2
CZ	4.18	2.95	1.73	1.22	2.45	1.73
DE	8.41	4.67	3.84	2.12	4.57	2.54
DK-E	1.97	0.58	0.87	0.25	1.10	0.33
DK-W	6.19	1.73	2.91	0.79	3.28	0.94
FI	0.59	0.08	0.16	0.02	0.43	0.06
FR	7.77	0.23	4.05	0.12	3.72	0.11
NL	0.98	0.34	0.51	0.18	0.47	0.16
NO1	1.31	0.00	0.00	0.00	1.31	0.00
NO2	66.90	0.00	37.65	0.00	29.25	0.00
NO5	127.45	0.00	84.98	0.00	42.47	0.00
PL	0.91	0.72	0.33	0.26	0.58	0.46
RO	0.24	0.06	0.07	0.02	0.17	0.04
SE1	1.06	0.00	0.47	0.00	0.59	0.00
SE2	10.62	0.00	5.02	0.00	5.60	0.00
SE3	6.67	0.09	3.04	0.04	3.63	0.05
SK	0.66	0.11	0.26	0.04	0.40	0.07
NCS3-B	3.37	0.00	4.95	0.00	-1.58	0.00
NCS4-B	222.85	0.00	180.70	0.00	42.15	0.00
NCS5-B	20.84	0.00	11.33	0.00	9.51	0.00

Table D.2: Yearly average CO₂-coefficients [ton CO₂/GWh] in partial- and full electrification.

Area	Scenario		Area	Scenario	
	Partial el.(2025)	Full el.(2025)		Partial el.(2025)	Full el.(2025)
AL	0.00	0.00	NL	343.77	345.53
AT	81.43	82.29	NO1	0.00	0.00
BA	792.01	792.68	NO2	0.00	0.00
BE	82.01	82.05	NO3	0.16	0.73
BG	409.19	409.29	NO4	0.02	0.08
CH	3.92	3.92	NO5	0.00	0.00
CZ	704.22	705.11	PL	785.96	787.93
DE	552.31	554.77	PT	56.56	56.57
DK-E	286.72	296.43	RO	249.15	249.47
DK-W	271.41	279.83	RS	802.42	802.78
EE	110.19	110.19	SE1	0.00	0.00
ES	176.60	177.19	SE2	0.00	0.00
FI	128.85	138.57	SE3	13.30	14.11
FR	29.52	29.79	SE4	0.00	0.00
GR	549.31	550.94	SI	326.25	326.75
HR	256.55	258.00	SK	164.95	165.26
HU	130.22	130.44	UK-N+UK-N-W	0.00	0.00
IE	335.78	336.38	UK-M+UK-M-W	0.00	0.00
IT	233.27	233.70	UK-S+UK-S-W	0.00	0.00
LT	186.95	186.96	NCS1	0.00	0.00
LU	81.14	81.04	NCS2	425.65	0.00
LV	151.03	151.54	NCS3	453.25	0.00
ME	609.44	610.06	NCS4	100.30	0.00
MK	439.95	439.95	NCS5	67.43	0.00
NI	168.69	168.94	NCS4	100.30	0.00
NL	343.77	345.53	NCS5	67.43	0.00

Appendix E

The PFT Model

The PFT Model is developed in Python and consists of two separate codes:

The PFT code and The Plot code.

(Pages 80-93)

(Restricted public access.)

